A Comprehensive Analysis of Strength-Based Optimum Signal Detection in Concentration-Encoded Molecular Communication With Spike Transmission

Mohammad Upal Mahfuz*, *Student Member, IEEE*, Dimitrios Makrakis, *Member, IEEE*, and Hussein T. Mouftah, *Fellow, IEEE*

***Abstract*—In this paper, a comprehensive analysis of strength-based optimum signal detection model has been presented for concentration-encoded molecular communication (CEMC) with spike (i.e., impulsive) transmission based on amplitude-shift keying (ASK) and on-off keying (OOK) modulations. Strength-based optimum signal detection problem in diffusion-based CEMC system has been investigated in detail in the presence of both diffusion noise and intersymbol interference (ISI). The receiver for optimum signal detection has been developed theoretically and explained with both analytical and simulation results of binary signal detection. Results show that the receiver thus developed can detect CEMC symbols effectively; however, the performance is influenced by three main factors, namely, communication range, transmission data rate, and receiver memory. For both ASK and OOK receivers, exact and approximate detection performances have been derived analytically depending on the probabilistic nature of molecular availability and the relationship between mean and variance of signal strengths. Correspondingly, bit error rate (BER) performance of the optimum receiver in a single CEMC link is further evaluated under various scenarios through extensive simulation experiments.**

***Index Terms*—Concentration-encoding, intersymbol interference, molecular communication, nanonetworks, optimum receiver, strength-based signal detection.**

I. Introduction

In recent years, research efforts on the interdisciplinary fields of nanotechnology, molecular and synthetic biology as well as information and communication engineering have brought about a remarkable progress in the area of nanomachine communication [1]–[7]. Molecular communication (MC) is now being considered as one of the promising techniques suitable for communication among bio-nanomachines [7], [8]. A generic MC system consists of a transmitting nanomachine (TN), a receiving nanomachine (RN) and a propagation channel between them [9], [10]. In diffusion-based MC, a TN releases information molecules[1] that undergo diffusion process based on random-walk motion [11] of the molecules in the propagation medium and thus reach an RN in a probabilistic manner [12]. In MC, information symbols can be transmitted by modulating several features of the molecules, e.g., specific type [13], concentration [14], transmission order [15], and release time [16] of molecules.

In concentration-encoded molecular communication (CEMC), a TN uses a single type of molecules to encode information [10]. The TN modulates the amplitude of the transmitting rate of molecules, and correspondingly, the RN decodes the information symbols by observing the intensity [17], [18] or the strength [17], [19] of concentration of molecules at the location of its receptors. Hence the detection schemes in CEMC are known as sampling-based [18] and strength-based [19], [20] detections respectively. In CEMC, the *intensity* and the *strength* of signal respectively mean the instantaneous amplitude of concentration of molecules at any time instant [14] and the total number of accumulated molecules in the entire symbol duration [14]. In this paper, concentration of molecules is explained in terms of the number of molecules per unit sensing volume of the receiver. Unlike sampling-based detection [18], in strength (i.e., energy)-based signal detection, the RN accumulates the received molecules during the entire symbol interval, produces a test statistic [20], [21] and decides based on its strength compared to a threshold. In CEMC, strength-based detection can equivalently be termed as energy-based detection (ED)[2] [22]. This is because concentration strength of a symbol is represented as the energy of the symbol in terms of the total number of accumulated molecules during that symbol [10], [22].

In ideal diffusion, the molecules propagate freely even after they first hit the RN, which causes intersymbol interference (ISI) by producing residual molecules that originate at the previously transmitted symbols but become available to the RN at the current symbol [10]. Therefore, in CEMC, the same type

Manuscript received February 18, 2014; revised June 09, 2014; accepted October 25, 2014. Date of publication January 13, 2015; date of current version February 27, 2015. M. U. Mahfuz would like to thank the Natural Sciences and Engineering Research Council of Canada (NSERC) for financial support in the form of PGS-D scholarship during the years 2010–2013. A small part of this paper was peer-reviewed, presented at, and published in the proceedings of BODYNETS-2013 conference in Boston, MA, USA, during 30 September to 02 October 2013, DOI: 10.4108/icst.bodynets.2013.253560. *Asterisk indicates corresponding author.*

*M. U. Mahfuz is with the School of Electrical Engineering and Computer Science, University of Ottawa, ON K1N6N5 Canada (e-mail: mmahf050@uottawa.ca).

D. Makrakis and H. T. Mouftah are with the School of Electrical Engineering and Computer Science, University of Ottawa, ON K1N6N5 Canada (e-mail: dimitris@eecs.uottawa.ca; mouftah@uottawa.ca).

Color versions of one or more of the figures in this paper are available online at http://ieeexplore.ieee.org.

Digital Object Identifier 10.1109/TNB.2014.2368593

[1]In the remainder of the paper, a "molecule" would mean an "information molecule" that is different from a fluid or solvent molecule.

[2]We use the term ED to denote strength-based detection in short and the subscript "$_{\mathrm{ED}}$" to denote the quantities related to strength-based signal detection in the later sections of this paper.

of molecules transmitted in different numbers to represent different transmitted symbols makes it difficult for the RN to distinguish the molecules intended for the current symbol from those intended for the previous symbols. When distance between TN and RN increases, the effects of ISI become severe because of the temporal spreading of the impulse response of the molecular channel [9], [10]. In addition, the effect of ISI increases when transmission data rate increases. As a result, optimum signal detection in CEMC is an extremely challenging problem.

In this paper, strength-based optimum detection of CEMC signals has been investigated in detail. A small part of this work has been published in [20] that reported the generalized model of strength-based signal detection in CEMC. More particularly, the work in [20] presented in a much limited manner a generalized model of strength-based CEMC signal detection in the presence of diffusion noise and ISI with generalized amplitude-shift keying (ASK) modulation with impulsive transmission only. In addition, the work in [20] did not consider the effects of ISI on the theoretical performance of the optimum detector, nor did it provide results of the optimum receiver in the presence of ISI. In addition, the work in [20] focused on ASK modulated scheme only. However, in this paper, we thoroughly expand the work on optimum receiver and its performance presented in [20].

The main contributions of this paper over its conference version [20] published previously are the following:

- The generalized optimum receiver model has been thoroughly extended for both ASK- and on-off keying (OOK)-based transmission schemes, with and without the effects of ISI. Signal detection models have been presented in detail in order to offer detection capabilities for both ASK- and OOK-modulated CEMC schemes.
- Detection performance of the optimum receiver has been derived theoretically with and without the effects of ISI. For the optimum receiver, the exact and the approximate detection performances have been derived analytically and explained in detail in two realistic scenarios where the optimum receiver can be built and analyzed with some level of approximation.
- The optimum receiver has been built in software by incorporating the effects of ISI-producing molecules at the RN by considering the memory capability of the RN. Correspondingly, bit error rate (BER) performance of the optimum receiver thus developed has been presented in detail when communication range, transmission data rate, and receiver memory vary. Based on receiver memory in the form of the number of previously decoded bits that the RN is capable of decoding correctly, three versions of the receiver have been investigated, and the corresponding BER characteristics have been evaluated.

1) Abbreviations:

ASK	Amplitude-shift keying.
BER	Bit error rate.
bps	Bits per second.
CEMC	Concentration-encoded molecular communication.
CIR	Channel impulse response.
FC	Full complexity.
ISI	Intersymbol interference.
MC	Molecular communication.
OOK	On-off keying.
RC	Reduced complexity.

2) List of Symbols:

D	Diffusion constant: 10^{-6} cm^2/s, i.e., 100 $\mu\mathrm{m}^2/\mathrm{s}$.
f	Transmission data rate.
$G(r,t)$	Energy-normalized CIR as sensed by the RN.
$n_{\mathrm{ED}}^{\mathrm{Noise}}$, $n_{\mathrm{ED}}^{\mathrm{ISI}}$	Diffusion noise and ISI quantities respectively.
$n_{\mathrm{ISI}}(t)$	Intensity of ISI-producing molecules.
M	Receiver memory size in unit of *symbol*.
N_{b}	Number of bits.
$p(r,t)$	Probability of getting a molecule in contact with RN at r and t.
P_{D}, P_{FA}	Probabilities of detection and false alarm respectively.
Q_0, Q_1	Number of transmitted molecules.
$Q(t)$	Input signal, i.e., transmission rate of molecules, in molecules/s.
r, t	TN-RN distance and time variables respectively.
$r_{\mathrm{BER}=0}$	Communication range up to which zero BER can be obtained.
$R_{\mu}^{(i)}$, $R_{\sigma}^{(i)}$	*Mean strength ratio* and *standard deviation strength ratio* of ISI-producing molecules to desired signal molecules respectively at hypothesis H_i.
$s_m(r,t)$	Mean concentration of molecules at r and t.
$s_{\mathrm{ED}}^{(i)}$, $\sigma_{\mathrm{S(ED)}}^{2(i)}$	Mean signal strength and variance of diffusion noise respectively under hypothesis H_i.
t_s	Sampling time interval.
T, T', T''	Test statistic.
T_{sym}	Symbol duration.
$U(r,t)$	Mean concentration of molecules, i.e., number of available molecules at r and t.
VRV	Virtual receive volume, approximately 1 $\mu\mathrm{m}^3$.
(x_r, y_r, z_r)	Location of the RN in Cartesian coordinate system.
$y(t)$, y_{ED}	Intensity and strength respectively perturbed by diffusion noise.
$z(t)$, z_{ED}	Intensity and strength respectively perturbed by diffusion noise and ISI.
x_{ED}	Standard normal variable $\mathcal{N}(0,1)$.
X, Y, Z	Axes in Cartesian coordinate system.

α	Ratio of amplitudes, i.e., $\alpha = (Q_1/Q_0)$.
$\gamma_{\mathrm{ED}}, \gamma'_{\mathrm{ED}}$	Threshold values.
$\mathcal{K}_{\mu}^{(i)}, \mathcal{K}_{\sigma}^{(i)}$	Constants related to mean and variance of $T''(H_i)$.
$\ell(z_{\mathrm{ED}} \mid \mathrm{H}_i)$	Conditional probabilities under hypothesis H_i.
$\mathcal{L}$	Limit operator.
τ_{DS}	Delay spread.
$\mathcal{N}(\mu, \sigma^2)$	Normal-distributed random variable with mean μ and variance σ^2.
χ_1^2	Chi-square random variable with 1 degree of freedom.
$\mathsf{Q}(.)$	Right tail probability.
∇^2	Laplacian operator.
$\Lambda^{(i)}$	Signal to diffusion-noise strength ratio.

The paper is organized as follows: Section II provides the related work, followed by Section III detailing the strength-based optimum signal detection in CEMC. Section IV presents a comprehensive analysis of the theoretical detection performances for ASK and OOK signal detections in CEMC respectively. Simulation results of the BER performance of the optimum and the suboptimum receivers have been presented in Section V. Finally, Section VI concludes the paper with a summary of the findings.

II. Related Work

Strength-based signal detection was first conceptualized in [17] that first proposed ED technique as a means to determine the effective communication ranges in CEMC between a pair of nanomachines. Later on, the idea of ED scheme was further investigated in [22] that provided threshold-based ED schemes in CEMC. On the other hand, taking into account the effects of stochastic ligand-receptor binding based on chemical Langevin equation [23], the ED scheme with mean concentration of molecules at the RN was later investigated in terms of performances depending on communication ranges and transmission rates [19] as well as variable threshold-based CEMC detection depending on stochastic chemical kinetics and receiver memory considerations [24]. However, the works presented in [17], [19], [22] were based on mean signal intensity only and did not consider diffusion-based noise [18] at the RN while developing the ED scheme.

The mechanism of energy-based signal detection in MC has also been investigated with communication metric-based approach in [25], however, without providing any performance evaluation in the form of information/detection theoretical or BER analyses.

A sequence detector-based receiver design for MC has been presented in [26] that focuses on high data rate MC and reports that sequence detectors can be possible at the expense of high computational complexity at the RN. Though sequence detection methods are widely seen in the traditional high-speed digital wireless communications, there is still inadequate evidence that such sequence detectors would be possible for MC, especially at high rates, given the fact that diffusion-based molecular propagation is an extremely slow process [7]. In addition, since nanomachines generally are of extremely low functional capacity [7], [8], it is not clear yet in the literature whether nanomachines would be able to implement such computationally intensive sequence detectors. Unlike [26], our work in this paper focuses on strength-based scalar symbol detection, and not signal vector detection, for low rate MC systems that are more biologically suitable, e.g., in calcium signaling [27], liver cells [28], and endocrine systems [29].

Apart from these, other related works include finding the optimum threshold-based detection with a prior signal transmission probability and without considering the diffusion noise as reported in [30], and in a noiseless scenario as in [30] but from the microscopic perspective with only one molecule transmitted as shown in [31]. In addition, optimum molecule-shift keying (MoSK) receiver was presented in [32], where the TN encodes information symbols in different types of information molecules. A signal detection scheme based on multiple amplitude modulation dealing with the diffusion channel from microscopic perspective, where the molecule with drift velocity is removed from the system once it hits the RN, has been reported in [33]. The work in [34] identified the noise in diffusion-based propagation of molecules as *particle-counting noise* and developed the expression of the concentration signal perturbed by the diffusion noise at the location of the RN.

Our work presented in this paper is different from the works presented in [30]–[33] in the sense that we consider the CEMC system from the macroscopic perspective dealing with the *concentration* of a large number of transmitted molecules, all of which are of a single type all through and the molecules propagate in an unbounded three-dimensional propagation medium. In our system model, none of the molecules is removed from the system upon its first hit at the RN, thereby providing an ideal (i.e., free) diffusion-based propagation environment. In addition, we also consider both diffusion noise and ISI in detail while developing the ED scheme in CEMC, which, to the best of our knowledge, were not incorporated in any of the available open literature including ours.

III. Strength-Based Optimum Signal Detection Model

As shown in Fig. 1, the TN and the RN communicate with a single type of information molecules that can bind with a single type of receptors located on the surface of the RN. The TN is a point source type transmitter and is located at the origin (0,0,0). In this paper, we consider two modulation schemes, namely, ASK and OOK, both based upon spike (i.e., impulsive) transmission.

1) ASK: In the generalized ASK-modulated scheme, the TN emits $Q_{b_j}\delta(t)$ information molecules in impulsive fashion at the beginning of each symbol[3] duration T_{sym}, where $b_j \in \{0,1\}$, $Q_{b_j} \gg 1$, and $\delta(t)$ denotes the Dirac delta function [35]. As a result, in a time-slotted fashion, the TN transmits Q_0 and Q_1 molecules at the beginning of each T_{sym} when it wants to transmit bit 0 and bit 1 respectively. Therefore, $\Sigma_{j=0}^{N_b-1} Q_{b_j}\delta(t - jT_{\mathrm{sym}})$ represents the transmitted signal, where $b_j \in \{0,1\}$, $j = \{1,2,\ldots,N_b\}$, is the bit to be transmitted, N_b is the total number of bits in the bit sequence.

[3]In binary system, each bit (0 or 1) represents one symbol. However, in Θ-ary system, each symbol consists of $\log_2 \Theta$ bits, Θ being the alphabet size [51].

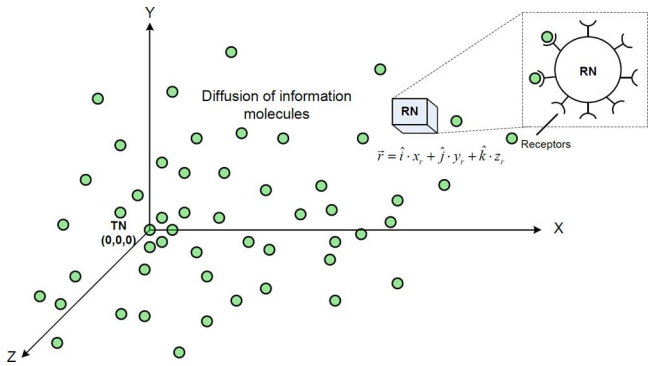

Fig. 1. Ideal (i.e., free) diffusion of information molecules (green circles) in three-dimensional unbounded propagation medium. The RN is located at the centre of the VRV. The receptors on the surface of the RN are shown in the inset.

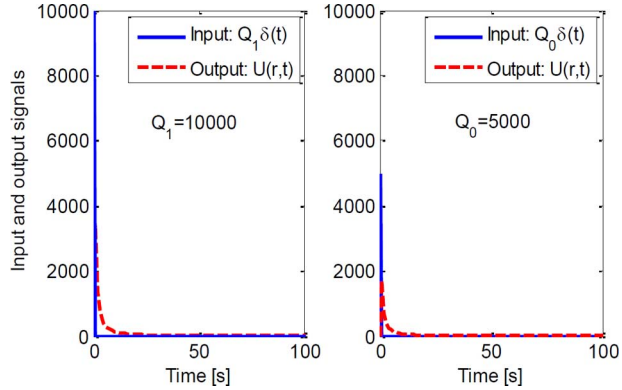

Fig. 2. Mean concentration signal intensity $U(r,t)$ at $r = 10$ μm in response to impulse transmissions $Q_1\delta(t)$ and $Q_0\delta(t)$ when bits 1 and 0 are transmitted respectively [20].

Hence $\mathbf{b} = [b_0, b_1, b_2, \ldots, b_{(N_b-1)}]$ denotes the bit sequence transmitted by the TN.

2) OOK: In the OOK-modulated scheme, in a time-slotted fashion, the TN emits Q_1 molecules at the beginning of each T_{sym} when it wants to transmit bit 1 and no molecules at all when it wants to transmit bit 0. As a result, the TN apparently remains "off" while bit 0 is being transmitted. OOK is a special case of ASK when $Q_0 = 0$.

The RN is assumed to be located at the centre of a small volume known as the *virtual receive volume* (VRV) [36]. VRV is a small unit volume [37] (e.g., 1 μm^3, which is the typical volume of a bacterium, i.e., a bionanomachine [8]) surrounding the RN where the RN senses the information molecules that are available at the RN and come in contact with its surface receptors. We consider a *perfect molecule monitor* that can estimate the concentration of molecules accurately [38], [39]. While information molecules can bind with the receptors with some probability based on the kinetic properties of molecule-receptor binding process (MRBP), we do not consider the MRBP in this paper. Rather we consider a sufficiently high density of receptors on the surface of the RN, which ensures that the available molecules on the surface of the RN come in contact with the receptors [40]. The TN and the RN are assumed to be in time-synchronization [4] and not move in space. Time-synchronization between the TN and the RN can be achieved by using external signals [41].

The concentration of molecules varies with time and space as below [12]

$$\frac{\partial U(r,t)}{\partial t} = D\nabla^2 U(r,t) \tag{1}$$

where $U(r,t)$ denotes the mean intensity of the concentration signal, in number of molecules per unit volume (e.g., per 1 μm^3), at the location of RN, r is the distance between the TN and the RN located at (x_r, y_r, z_r) where $r^2 = x_r^2 + y_r^2 + z_r^2$ when Cartesian coordinate system is assumed, t is the time variable, D is the diffusion constant of information molecules in the three-dimensional unbounded propagation medium, and ∇^2 is the three-dimensional Laplacian operator denoted as $\partial^2/\partial x^2 + \partial^2/\partial y^2 + \partial^2/\partial z^2$. In response to an impulsive transmission, $Q_m\delta(t)$, the output signal $U(r,t)$ can be defined as the channel impulse response (CIR) expressed as $G(r,t)$ shown below.

$$U(r,t) = \frac{Q_m}{(4\pi Dt)^{3/2}} e^{-r^2/4Dt} \triangleq G(r,t). \tag{2}$$

Fig. 2 shows the mean CIR of the molecular channel. Within the VRV, the mean concentration of the information molecules available to the RN can be expressed as below [18].

$$\begin{aligned} s_m(r,t) &= \frac{1}{\text{VRV}} \iiint_{\text{VRV}} \frac{Q_m}{(4\pi Dt)^{3/2}} e^{-(x_r^2+y_r^2+z_r^2)/4Dt} dX dY dZ \\ &= Q_m p(r,t) \end{aligned}$$

where

$$p(r,t) = \frac{1}{\text{VRV}} \iiint_{\text{VRV}} \frac{1}{(4\pi Dt)^{3/2}} e^{-(x_r^2+y_r^2+z_r^2)/4Dt} dX dY dZ. \tag{3}$$

Here $dV = dX dY dZ$ is the differential volume in the VRV and $p(r,t)$ is the probability of getting one molecule [12], [18] in the VRV. As shown in (3), mean concentration inside the VRV is determined by integrating the mean CIR $G(r,t)$ with respect to the VRV and dividing by the VRV. In CEMC, the number of molecules that the RN and the TN handles is large and it is, therefore, convenient to consider concentration[4] in the encoding and decoding of the message [8]. For simplicity of analysis [42], in this paper, we consider a perfect molecule monitor [38], [39], which from (3) provides that the mean intensity of concentration signal within the VRV (1 μm^3) of the RN is $s_m(r,t) = G(r,t)$. Also note that, in this paper in all the results except those in Fig. 10, we consider sampling time intervals of $t_s = 1$ second (s), which is quite reasonable to ensure that any two samples of concentration intensity are statistically independent and provide options for the RN to make an accurate measurement of concentration [38], [39], [43].

Note here that RN samples the concentration intensity of molecules at uniform temporal intervals of t_s s and works on the basis of energy normalization principle explained in detail in our previous works [18], [44]. For various sampling rates that the RN can adopt, in most cases in short, medium, and long communication ranges [10], $p(r,t)$ varies in the range $0 \leq p(r,t) \leq 0.5$; see Fig. 11 in Appendix B [18], [44]. Since each of the $Q_m \gg 1$ transmitted molecules travels independently in the unbounded three-dimensional space, the

[4]Concentration refers to the number of molecules per unit volume, e.g., per 1 μm^3, which is equal to the VRV in our case.

number of molecules available at the RN at any time instant due to diffusion only is a random variable $y(t)$ and, based on the normal-approximation to the binomial distribution, can be expressed as below [8], [18], [32], [37].

$$\begin{aligned} y(t) &\sim \mathcal{N}\left(s_m(t), s_m(t)(1-p(t))\right) \\ \Rightarrow y(t) &= s_m(t) + n_{\text{samp}}(t) \\ &\text{where} \\ n_{\text{samp}}(t) &\sim \mathcal{N}\left(0, s_m(t)(1-p(t))\right). \end{aligned} \tag{4}$$

Here $n_{\text{samp}}(t)$ denotes the diffusion noise at the sample taken at the time instant t and $\mathcal{N}(\mu_\vartheta, \sigma_\vartheta^2)$ denotes a normal-distributed random variable ϑ with mean μ_ϑ and variance σ_ϑ^2. For simplicity in writing the equations, at a given r, the functional dependences of $s_m(r,t)$ and $p(r,t)$ on r are omitted and so hereafter the respective quantities are shown as functions of t only, i.e., $s_m(t)$ and $p(t)$.

In ED scheme, after the RN has sensed the concentration samples at its receptors at regular time intervals of t_s s, it produces a resultant concentration available at the RN during that symbol. As a result, the output variable (i.e., test statistic) of strength-based detection scheme in diffusion noise only can be expressed as below, where N_{samp} denotes the number of samples per symbol.

$$\begin{aligned} y_{\text{ED}} &= \sum_{n=0}^{N_{\text{samp}}} t_s y(nt_s) \Rightarrow y_{\text{ED}} \sim \mathcal{N}\left(s_{\text{ED}}, \sigma^2_{\text{S(ED)}}\right) \text{ where} \\ s_{\text{ED}} &= \sum_{n=0}^{N_{\text{samp}}} t_s s_m(nt_s) \text{ and} \\ \sigma^2_{\text{S(ED)}} &= \sum_{n=0}^{N_{\text{samp}}} t_s^2 s_m(nt_s)\left(1-p(nt_s)\right). \end{aligned} \tag{5}$$

Therefore,

$$\begin{aligned} y_{\text{ED}} &= s_{\text{ED}} + n_{\text{ED}}^{\text{Noise}} \text{ where} \\ n_{\text{ED}}^{\text{Noise}} &\sim \mathcal{N}\left(0, \sigma^2_{\text{S(ED)}}\right) = \sigma_{\text{S(ED)}}\mathcal{N}(0,1). \end{aligned} \tag{6}$$

Note that (5) is valid only when the temporal samples of concentration intensity are uncorrelated and statistically independent, which can be ensured by choosing the t_s reasonably larger than the waiting time of a molecule in sensing volume VRV, e.g., 1 μm^3, of the RN [38]. In this paper, we choose $t_s = 1$ s that satisfies both the condition of sampling time of statistically independent, uncorrelated samples and its biological relevance to measurement intervals for bionanomachines, e.g., *E. Coli* [38]. Since biological nanomachines are generally very limited in their functionalities and are able to perform simple computational tasks only [5], [8], it is highly desired to keep a low computational burden on the RN. When the number of samples increases, as shown in (5), it correspondingly increases the receiver circuit complexity and so the computational burden on the RN. Therefore, given the extremely limited functional capacity of the RN [5], [8], i.e., a biological nanomachine [8], the RN would most likely not be able to build a highly complicated detection circuitry within itself. Therefore, we focus our attention to more realistic scenarios by using a fixed sampling time interval ≥ 1 s. On the other hand, N_{samp} depends on the data rate f and the sampling time interval t_{s} of the system and can be expressed as $N_{\text{samp}} = 1/(ft_{\text{s}})$.

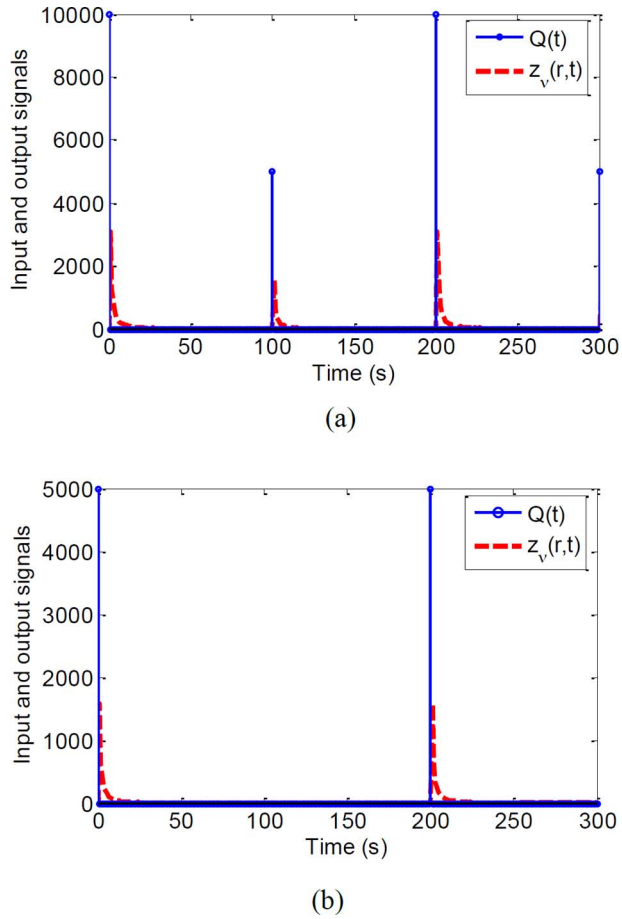

Fig. 3. Input $Q(t)$ and one realization $z_v(t)$ of the output signal at $r = 10$ μm in (a) binary ASK and (b) OOK CEMC systems with diffusion noise and ISI, where $T_{\text{sym}} = 100$ s and transmitted bits are $\{1010\ldots\}$. (a) ASK: $Q_1 = \alpha Q_0$ when $Q_0 = 5000$ and $\alpha = 2$ [20]. (b) OOK: $Q_1 = 5000$ and $Q_0 = 0$.

In the accumulated molecules during the i-th symbol, in addition to the molecules that were intended for the i-th symbol only, the RN would also receive some of the molecules that were not intended for the i-th symbol. This means some of the molecules that were transmitted during the first to the $(i-1)^{-\text{th}}$ symbols would become available at the RN during the $i^{-\text{th}}$ symbol, causing ISI to the $i^{-\text{th}}$ symbol. Therefore, the intensity $z(t)$ and the strength z_{ED} of the CEMC signal including the effects of ISI can be written as

$$z(t) = y(t) + n_{\text{ISI}}(t) \Rightarrow z_{\text{ED}} = s_{\text{ED}} + n_{\text{ED}}^{\text{Noise}} + n_{\text{ED}}^{\text{ISI}} \tag{7}$$

where $n_{\text{ED}}^{\text{Noise}}$ is as shown in (6) and $n_{\text{ED}}^{\text{ISI}}$ denotes the resultant concentration of residual molecules causing ISI. Since the concentration *intensity* [14] at any time instant t is a normal-distributed random variable [18] and concentration *strength* can be found as the integral of concentration intensity over the symbol duration [14], $n_{\text{ED}}^{\text{ISI}}$ can also be expressed as a normal-distributed random variable as $n_{\text{ED}}^{\text{ISI}} \sim \mathcal{N}(\mu_{\text{ISI(ED)}}, \sigma^2_{\text{ISI(ED)}})$. Fig. 3 shows the input signal and v-th realization $z_v(t)$ of the output signal $z(t)$. Therefore, strength-based binary detection problems in ASK- and OOK-modulated CEMC systems can be formally

written as below, where hypotheses H_1 and H_0 denote the cases when bits 1 and 0 are to be transmitted respectively.

$$\text{ASK:} z_{\mathrm{ED}} = \begin{cases} \mathcal{N}\left(s_{\mathrm{ED}}^{(1)} + \mu_{\mathrm{ISI(ED)}}, \sigma_{\mathrm{S(ED)}}^{2(1)} + \sigma_{\mathrm{ISI(ED)}}^{2}\right); & \mathrm{H}_1 \\ \mathcal{N}\left(s_{\mathrm{ED}}^{(0)} + \mu_{\mathrm{ISI(ED)}}, \sigma_{\mathrm{S(ED)}}^{2(0)} + \sigma_{\mathrm{ISI(ED)}}^{2}\right); & \mathrm{H}_0 \end{cases} \tag{8a}$$

$$\text{OOK:} z_{\mathrm{ED}} = \begin{cases} \mathcal{N}\left(s_{\mathrm{ED}}^{(1)} + \mu_{\mathrm{ISI(ED)}}, \sigma_{\mathrm{S(ED)}}^{2(1)} + \sigma_{\mathrm{ISI(ED)}}^{2}\right); & \mathrm{H}_1 \\ \mathcal{N}\left(\mu_{\mathrm{ISI(ED)}}, \sigma_{\mathrm{ISI(ED)}}^{2}\right); & \mathrm{H}_0. \end{cases} \tag{8b}$$

IV. Strength-Based Optimum Receivers

A. Optimum ASK Receiver Architecture

In this section, the optimum ASK receiver is developed first in Sections IV-A–IV-C, followed by the development of the optimum OOK receiver in Section IV-D. An optimum receiver provides the minimum probability of error in detecting the transmitted bits. Therefore, we consider Neyman-Pearson theorem [21] and calculate the logarithm of the likelihood ratio under the *minimum probability of error criterion* using equal prior probabilities $\Pr(\mathrm{H}_0) = \Pr(\mathrm{H}_1)$ in order to derive the test statistic $T(z_{\mathrm{ED}})$ as shown below

$$\frac{\ell\left(z_{\mathrm{ED}} \mid \mathrm{H}_1\right)}{\ell\left(z_{\mathrm{ED}} \mid \mathrm{H}_0\right)} > 1 \Rightarrow \ln \frac{\ell\left(z_{\mathrm{ED}} \mid \mathrm{H}_1\right)}{\ell\left(z_{\mathrm{ED}} \mid \mathrm{H}_0\right)} > 0 \tag{9}$$

where, for ASK system, the conditional probabilities can be expressed as shown below.

$$\ell\left(z_{\mathrm{ED}} \mid \mathrm{H}_1\right) = \frac{1}{\sqrt{2\pi\left(\sigma_{\mathrm{S(ED)}}^{2(1)} + \sigma_{\mathrm{ISI(ED)}}^{2}\right)}} \times \exp\left[-\frac{\left\{z_{\mathrm{ED}} - \left(s_{\mathrm{ED}}^{(1)} + \mu_{\mathrm{ISI(ED)}}\right)\right\}^2}{2\left(\sigma_{\mathrm{S(ED)}}^{2(1)} + \sigma_{\mathrm{ISI(ED)}}^{2}\right)}\right]$$

$$\ell\left(z_{\mathrm{ED}} \mid \mathrm{H}_0\right) = \frac{1}{\sqrt{2\pi\left(\sigma_{\mathrm{S(ED)}}^{2(0)} + \sigma_{\mathrm{ISI(ED)}}^{2}\right)}} \times \exp\left[-\frac{\left\{z_{\mathrm{ED}} - \left(s_{\mathrm{ED}}^{(0)} + \mu_{\mathrm{ISI(ED)}}\right)\right\}^2}{2\left(\sigma_{\mathrm{S(ED)}}^{2(0)} + \sigma_{\mathrm{ISI(ED)}}^{2}\right)}\right]. \tag{10}$$

The strength-based detector computes the test statistic $T(z_{\mathrm{ED}})$ at the end of symbol duration after the RN has produced a resultant concentration of all the molecules sensed during that symbol. Therefore, in each symbol the detection processing unit of the RN would generate one observation of $T(z_{\mathrm{ED}})$ and the detection of the symbol would be based on that observation. Combining (9) and (10) and simplifying yields the test statistic for ASK system as follows. See equation (11) at the bottom of the page.

As a result, the strength-based optimum receiver can be shown in Fig. 4. The main difference between a conventional energy-detector in EM wave-based signals and the strength-based detector in CEMC signals is that in CEMC the numbers of molecules causing diffusion noise and ISI depend on the signal value itself under the specific hypothesis. This makes the strength-based detection of CEMC signals and its receiver implementation significantly challenging. However, the detection models presented in this paper are able to provide theoretical performance and numerical simulation results that describe the BER performance of the optimum receiver in CEMC as well as the effects of any suitable simplifications that may be possible in the detection signal processing unit of the RN.

B. Optimum ASK Receiver (Exact Detection Performance)

In this subsection, we derive the exact detection performance of the *optimum ASK receiver* first, followed by its approximate detection performance, which leads to the *suboptimum ASK receiver* in the next subsection. Dividing both sides of (11) yields the following.

$$\frac{T(z_{\mathrm{ED}})}{a_{\mathrm{ED}}} = z_{\mathrm{ED}}^2 + c_{\mathrm{ED}} z_{\mathrm{ED}} - \gamma'_{\mathrm{ED}} \underset{\text{Select } \mathrm{H}_0}{\overset{\text{Select } \mathrm{H}_1}{\gtrless}} 0 \tag{12}$$

$$T\left(z_{\mathrm{ED}}\right) = a_{\mathrm{ED}} z_{\mathrm{ED}}^2 + b_{\mathrm{ED}} z_{\mathrm{ED}} - \gamma_{\mathrm{ED}} \underset{\text{Select } \mathrm{H}_0}{\overset{\text{Select } \mathrm{H}_1}{\gtrless}} 0, \text{ where}$$

$$a_{\mathrm{ED}} = \left\{\frac{1}{2\left(\sigma_{\mathrm{S(ED)}}^{2(0)} + \sigma_{\mathrm{ISI(ED)}}^{2}\right)} - \frac{1}{2\left(\sigma_{\mathrm{S(ED)}}^{2(1)} + \sigma_{\mathrm{ISI(ED)}}^{2}\right)}\right\}$$

$$b_{\mathrm{ED}} = \left\{\frac{\left(s_{\mathrm{ED}}^{(1)} + \mu_{\mathrm{ISI(ED)}}\right)}{\left(\sigma_{\mathrm{S(ED)}}^{2(1)} + \sigma_{\mathrm{ISI(ED)}}^{2}\right)} - \frac{\left(s_{\mathrm{ED}}^{(0)} + \mu_{\mathrm{ISI(ED)}}\right)}{\left(\sigma_{\mathrm{S(ED)}}^{2(0)} + \sigma_{\mathrm{ISI(ED)}}^{2}\right)}\right\}$$

$$-\gamma_{\mathrm{ED}} = \left\{\frac{1}{2}\ln\frac{\left(\sigma_{\mathrm{S(ED)}}^{2(0)} + \sigma_{\mathrm{ISI(ED)}}^{2}\right)}{\left(\sigma_{\mathrm{S(ED)}}^{2(1)} + \sigma_{\mathrm{ISI(ED)}}^{2}\right)} - \frac{\left(s_{\mathrm{ED}}^{(1)} + \mu_{\mathrm{ISI(ED)}}\right)^2}{2\left(\sigma_{\mathrm{S(ED)}}^{2(1)} + \sigma_{\mathrm{ISI(ED)}}^{2}\right)} + \frac{\left(s_{\mathrm{ED}}^{(0)} + \mu_{\mathrm{ISI(ED)}}\right)^2}{2\left(\sigma_{\mathrm{S(ED)}}^{2(0)} + \sigma_{\mathrm{ISI(ED)}}^{2}\right)}\right\}. \tag{11}$$

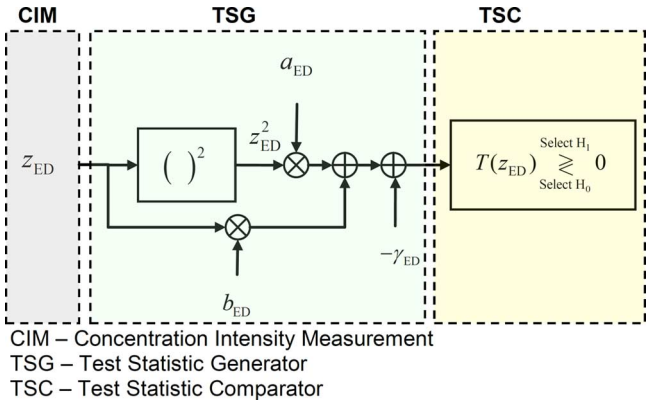

Fig. 4. Strength-based optimum receiver architecture in binary CEMC system with diffusion noise and ISI. The selection of the quantities $a_{\rm ED}$, $b_{\rm ED}$, and $\gamma_{\rm ED}$ determines the type of the receiver, i.e., ASK or OOK.

where $c_{\rm ED} = b_{\rm ED}/a_{\rm ED}$ and $\gamma'_{\rm ED} = \gamma_{\rm ED}/a_{\rm ED}$. At $\rm H_0$, since $z_{\rm ED} \sim \mathcal{N}\left(s_{\rm ED}^{(0)} + \mu_{\rm ISI(ED)}, \sigma^{2(0)}_{\rm S(ED)} + \sigma^2_{\rm ISI(ED)}\right)$, by converting $z_{\rm ED}$ into a standard normal variable $x_{\rm ED} \sim \mathcal{N}(0,1)$, i.e., $z_{\rm ED} = \left(s_{\rm ED}^{(0)} + \mu_{\rm ISI(ED)}\right) + \sqrt{\sigma^{2(0)}_{\rm S(ED)} + \sigma^2_{\rm ISI(ED)}}\,(x_{\rm ED})$, the data dependent terms of $T(z_{\rm ED})/a_{\rm ED}$, as shown in (12), yields the following modified test statistic $T'(z_{\rm ED})$ as shown below.

$$T'(z_{\rm ED}) = z_{\rm ED}^2 + c_{\rm ED} z_{\rm ED} \underset{\text{Select H}_0}{\overset{\text{Select H}_1}{\gtrless}} \gamma'_{\rm ED}. \tag{13}$$

Plugging the expression of $z_{\rm ED}$ as a function of $x_{\rm ED}$ into (13) and simplifying the results further yields the modified test statistic $T''(z_{\rm ED})$ as shown below.

$$T''(z_{\rm ED}) = \frac{T'(z_{\rm ED})}{\sigma^{2(0)}_{\rm S(ED)} + \sigma^2_{\rm ISI(ED)}} \sim \mathcal{N}\left(\mu_{T''(\rm H_0)}, \sigma^2_{T''(\rm H_0)}\right) + \chi_1^2$$

where

$$\mu_{T''(\rm H_0)} = \frac{\left(s_{\rm ED}^{(0)} + \mu_{\rm ISI(ED)}\right)\left(s_{\rm ED}^{(0)} + \mu_{\rm ISI(ED)} + c_{\rm ED}\right)}{\left(\sigma^{2(0)}_{\rm S(ED)} + \sigma^2_{\rm ISI(ED)}\right)}$$

and

$$\sigma^2_{T''(\rm H_0)} = \frac{4\left(s_{\rm ED}^{(0)} + \mu_{\rm ISI(ED)}\right)^2 + c_{\rm ED}^2}{\left(\sigma^{2(0)}_{\rm S(ED)} + \sigma^2_{\rm ISI(ED)}\right)}. \tag{14}$$

Here χ_1^2 is a chi-square distributed random variable with one degree of freedom with mean and variance equal to 1 and 2 respectively [21]. The expression of $T''(z_{\rm ED})$ in terms of the data-dependent terms is important because it will show the dominance of the normal distributed part over the chi-square distributed part, as will be shown later.

Similarly, it can be shown that, at $\rm H_1$, the test statistic can be found as the following.

$$T''(z_{\rm ED}) = \frac{T'(z_{\rm ED})}{\sigma^{2(1)}_{\rm S(ED)} + \sigma^2_{\rm ISI(ED)}} \sim \mathcal{N}\left(\mu_{T''(\rm H_1)}, \sigma^2_{T''(\rm H_1)}\right) + \chi_1^2$$

where

$$\mu_{T''(\rm H_1)} = \frac{\left(s_{\rm ED}^{(1)} + \mu_{\rm ISI(ED)}\right)\left(s_{\rm ED}^{(1)} + \mu_{\rm ISI(ED)} + c_{\rm ED}\right)}{\left(\sigma^{2(1)}_{\rm S(ED)} + \sigma^2_{\rm ISI(ED)}\right)}$$

and

$$\sigma^2_{T''(\rm H_1)} = \frac{4\left(s_{\rm ED}^{(1)} + \mu_{\rm ISI(ED)}\right)^2 + c_{\rm ED}^2}{\left(\sigma^{2(1)}_{\rm S(ED)} + \sigma^2_{\rm ISI(ED)}\right)}. \tag{15}$$

Therefore, by using the explanation and the justification provided in Appendix A, it can be shown that, in (14) and (15), the effects of χ_1^2 on $T''(z_{\rm ED})$ can be neglected and the test statistic can be simplified as below

$$T''(z_{\rm ED}) \sim \begin{cases} \mathcal{N}\left(\mu_{T''(\rm H_0)}, \sigma^2_{T''(\rm H_0)}\right), & \rm H_0 \\ \mathcal{N}\left(\mu_{T''(\rm H_1)}, \sigma^2_{T''(\rm H_1)}\right), & \rm H_1 \end{cases} \tag{16}$$

where the quantities are as described earlier. As a result, the probability of false alarm $(P_{\rm FA})$ can be obtained as follows.

$$\begin{aligned} P_{\rm FA} &= \Pr\{T'(z_{\rm ED}) > \gamma'_{\rm ED}; \rm H_0\} \\ &= \Pr\left\{T''(z_{\rm ED}) > \frac{\gamma'_{\rm ED}}{\sigma^{2(0)}_{\rm S(ED)} + \sigma^2_{\rm ISI(ED)}};\ \rm H_0\right\} \\ \Rightarrow \gamma'_{\rm ED} &= \left(\mathbf{Q}^{-1}(P_{\rm FA})\sigma_{T''(\rm H_0)} + \mu_{T''(\rm H_0)}\right)\left(\sigma^{2(0)}_{\rm S(ED)} + \sigma^2_{\rm ISI(ED)}\right). \end{aligned} \tag{17}$$

Here $\mathbf{Q}(.)$ denotes the right tail probability that can be expressed as $\mathbf{Q}(\zeta) = \int_\zeta^\infty (1/\sqrt{2\pi})\exp(-x^2/2)dx$ [21] and $\mathbf{Q}^{-1}(.)$ is the inverse of $\mathbf{Q}(.)$. Therefore, the exact expression of the probability of detection $(P_{\rm D})$ of the optimum ASK receiver can be found as the following. See equation (18) at the bottom of the page.

$$\begin{aligned} P_{\rm D} &= \Pr\{T'(z_{\rm ED}) > \gamma'_{\rm ED}; \rm H_1\} \\ &= \Pr\left\{T''(z_{\rm ED}) > \frac{\gamma'_{\rm ED}}{\sigma^{2(1)}_{\rm S(ED)} + \sigma^2_{\rm ISI(ED)}}; \rm H_1\right\} \\ &= \mathbf{Q}\left(\frac{\mathbf{Q}^{-1}(P_{\rm FA})\sigma_{T''(\rm H_0)} + \mu_{T''(\rm H_0)}}{\sigma_{T''(\rm H_1)}}\left(\frac{\sigma^{2(0)}_{\rm S(ED)} + \sigma^2_{\rm ISI(ED)}}{\sigma^{2(1)}_{\rm S(ED)} + \sigma^2_{\rm ISI(ED)}}\right) - \frac{\mu_{T''(\rm H_1)}}{\sigma_{T''(\rm H_1)}}\right). \end{aligned} \tag{18}$$

Signal-dependent means and variances of $T''(z_{\rm ED})$ as shown in (14) and (15) result in the complicated structure of the detection performance of the optimum receiver as shown in (18). Even if the chi-square term χ_1^2 can be ignored in the expression of $T''(z_{\rm ED})$ as shown in (16), regardless of whether the impact of ISI is significant in the system or not, deriving the detection performance from (18) is very difficult and it may not be feasible to derive a simpler structure of the detection performance in this case. Hence effort has been made to simplify the exact detection performance with reasonable approximations as shown next.

C. Suboptimum ASK Receiver

To develop suboptimum receiver, two scenarios have been considered, the first one, *Scenario 1*, being the most general in nature has been shown in this subsection, and the second one, *Scenario 2*, which can be derived from the first one, is shown in Appendix B. At each temporal instant, the ratio of mean signal intensity to its variance can be expressed as $s(t)/\{s(t)(1-p(t))\} = 1/(1-p(t))$ [18] where, as mentioned in Section III and Appendix B, for a receiver that samples the concentration intensity at intervals of t_s s, $p(t)$ varies in the range $0 \leq p(t) \leq 0.5$, the higher value of $p(t)$ occurring at the shorter communication ranges. Referring to (2)–(4), the quantity $1/(1-p(t))$ varies from ≈ 1 (when $p(t) \to 0$, e.g., at comparatively longer communication ranges or at long temporal instants) to ≈ 2 (when $p(t) \to 0.5$, e.g., at comparatively shorter communication ranges or at earlier temporal instants) [18]. In the most general form, no assumption is imposed on the value of $p\,(t)$, i.e., $p\,(t) \neq 0$ and so the results obtained in this subsection can be applied to all communication ranges, including long-range CEMC. However, at long communication ranges and/or long temporal instants with $T_{\rm obs} \to \infty$, $p(t) \approx 0$ can also be considered as an additional assumption that offers possible simplifications in the expression of $P_{\rm D}$, as shown in Appendix B.

In general, when $\mu_{\rm ISI} \ll s_{\rm ED}^{(i)}$, $\sigma^2_{\rm ISI(ED)} \ll \sigma^{2(i)}_{\rm S(ED)}$, $i \in \{0,1\}$, and from (5) $s_{\rm ED}^{(1)} = \alpha s_{\rm ED}^{(0)}$ and $\sigma^{2(1)}_{\rm S(ED)} = \alpha\sigma^{2(0)}_{\rm S(ED)}$, this results in $c_{\rm ED}$ not exactly equal to zero but $c_{\rm ED} \approx 0$, and at the same time, $c_{\rm ED} \ll s_{\rm ED}^{(i)} + \mu_{\rm ISI(ED)}$, where $i \in \{0,1\}$ denotes the index of hypothesis $\rm H_i$ shown in the subscript. This in turn provides a more general case when the mean and the variance of signal strength at $\rm H_0$ and $\rm H_1$ are not approximately equal, i.e., $s_{\rm ED}^{(0)} \neq \sigma^{2(0)}_{\rm S(ED)}$, $s_{\rm ED}^{(1)} \neq \sigma^{2(1)}_{\rm S(ED)}$, and $\mu_{\rm ISI(ED)} \neq \sigma^2_{\rm ISI(ED)}$.

Therefore, at $\rm H_0$, from (14) we get the mean and the variance of the test statistic as the following.

$$\mu_{T''(\rm H_0)} = \frac{\left(s_{\rm ED}^{(0)} + \mu_{\rm ISI(ED)}\right)^2}{\sigma^{2(0)}_{\rm S(ED)} + \sigma^2_{\rm ISI(ED)}}$$

and

$$\sigma^2_{T''(\rm H_0)} = \frac{4\,\left(s_{\rm ED}^{(0)} + \mu_{\rm ISI(ED)}\right)^2}{\sigma^{2(0)}_{\rm S(ED)} + \sigma^2_{\rm ISI(ED)}}. \tag{19}$$

Similarly, at $\rm H_1$, from (15), we get the corresponding quantities as the following.

$$\mu_{T''(\rm H_1)} = \frac{\left(s_{\rm ED}^{(1)} + \mu_{\rm ISI(ED)}\right)^2}{\sigma^{2(1)}_{\rm S(ED)} + \sigma^2_{\rm ISI(ED)}}$$

and

$$\sigma^2_{T''(\rm H_1)} = \frac{4\left(s_{\rm ED}^{(1)} + \mu_{\rm ISI(ED)}\right)^2}{\sigma^{2(1)}_{\rm S(ED)} + \sigma^2_{\rm ISI(ED)}}. \tag{20}$$

Following a similar procedure as shown in Section IV-B, by using (19), the threshold $\gamma'_{\rm ED}$ can be obtained as follows.

$$\gamma'_{\rm ED} = 2\mathbf{Q}^{-1}(P_{\rm FA})\left(s_{\rm ED}^{(0)} + \mu_{\rm ISI(ED)}\right)\sqrt{\sigma^{2(0)}_{\rm S(ED)} + \sigma^2_{\rm ISI(ED)}} + \left(s_{\rm ED}^{(0)} + \mu_{\rm ISI(ED)}\right)^2. \tag{21}$$

Therefore, using (20) and (21), $P_{\rm D}$ of the suboptimum ASK receiver can be obtained as below. See equation (22) at the bottom of the page.

Here, $R_\mu^{(i)}$ and $R_\sigma^{(i)}$ are the *mean strength ratio* and the *standard deviation strength ratio* of ISI-producing molecules to desired signal molecules respectively at a specific hypothesis. As shown in (22), $P_{\rm D}$ depends on $P_{\rm FA}$, α, $\Lambda^{(0)}$, $R_\mu^{(i)}$, and $R_\sigma^{(i)}$, $i \in \{0,1\}$. Keeping $P_{\rm FA}$, $R_\mu^{(i)}$, $R_\sigma^{(i)}$, $i \in \{0,1\}$, and $\Lambda^{(0)}$ fixed, when α increases, the argument of $\mathbf{Q}(.)$ in the right side of (22) decreases and so $P_{\rm D}$ increases. The effects of increasing the strength factor α is shown in Section IV-E. An increase in any one or more of $P_{\rm FA}$, α, and $\Lambda^{(0)}$ decreases the argument of $\mathbf{Q}(.)$ in (22), hence increases $P_{\rm D}$. These three quantities are

$$P_{\rm D} = \mathbf{Q}\left(\frac{\mathbf{Q}^{-1}(P_{\rm FA})}{\alpha^{3/2}}\left(\frac{1+R_\mu^{(0)}}{1+R_\mu^{(1)}}\right)\sqrt{\frac{1+\left(R_\sigma^{(0)}\right)^2}{1+\left(R_\sigma^{(1)}\right)^2}} - \frac{\Lambda^{(0)}}{2}\left\{\frac{\alpha^2\left(1+R_\mu^{(1)}\right)^2 - \left(1+R_\mu^{(0)}\right)^2}{\alpha^{3/2}\left(1+R_\mu^{(1)}\right)\sqrt{1+(R_\sigma^{(1)})^2}}\right\}\right)$$

$$\text{where } \Lambda^{(0)} = \frac{s_{\rm ED}^{(0)}}{\sigma^{(0)}_{\rm S(ED)}}, R_\mu^{(i)} = \frac{\mu_{\rm ISI(ED)}}{s_{\rm ED}^{(i)}}, R_\sigma^{(i)} = \frac{\sigma_{\rm ISI(ED)}}{\sigma^{(i)}_{\rm S(ED)}}, i \in \{0,1\}. \tag{22}$$

either related to transmission or detection systems and diffusion-based noise, but not related to ISI-producing molecules.

On the other hand, the quantities $R_\mu^{(i)}$ and $R_\sigma^{(i)}$ indicate the effects of ISI-producing molecules at the current symbol. Note that $R_\mu^{(i)}$ and $R_\sigma^{(i)}$ also depend on the mean signal strength and the variance of diffusion-noise respectively, as mentioned earlier in (22). Therefore, expressing the effects of ISI at the current symbol in terms of signal-dependent quantities can be considered as a convenient way to illustrate the effects of ISI by varying the quantities $R_\mu^{(i)}$ and $R_\sigma^{(i)}$, $i \in \{0,1\}$. As mentioned earlier, signal-dependence of diffusion-noise and ISI makes the CEMC signal detection extremely challenging. Therefore, (22) provides the system designer with a useful expression to study the effects of ISI on $P_{\rm D}$ as well as a means to distinguish the role of ISI from that of diffusion-based noise in the system. For instance, in the absence of ISI, plugging $R_\mu^{(i)} = 0$ and $R_\sigma^{(i)} = 0$, $i \in \{0,1\}$ in (22) provides the detection performance without the effects of ISI.

D. Suboptimum OOK Receiver

In this subsection, we extend the detection of ASK system to OOK scheme. The derivation of optimum OOK receiver follows a similar procedure shown in Sections IV-A–IV-C. Note that, for an OOK system, considering $s_{\rm ED}^{(0)} = 0$ and $\sigma_{\rm S(ED)}^{2(0)} = 0$ in (11)–(15) and following a similar procedure as shown in Section IV-C yield the detection performance of the suboptimum OOK receiver in *Scenario 1* as the following. See equation (23) at the bottom of the page.

The detection performance of the OOK receiver can be explained in a similar way as shown earlier in terms of $P_{\rm FA}$, $\Lambda^{(1)}$, $R_\mu^{(1)}$, and $R_\sigma^{(1)}$.

E. Analytical Results

Since $P_{\rm D}$ is affected by the signal and ISI-related quantities as well as diffusion-noise, for various signal strengths, ISI strengths, and diffusion-noise variances, the achievable $P_{\rm D}$ would change accordingly. For instance, when ISI-producing molecules from one or more of the previous bits become available at the RN, $P_{\rm D}$ decreases. In this relation, we consider two cases, namely, when 1 and 5 previous bits cause ISI at the current bit. Fig. 5 shows the characteristics of the quantities related to signal and ISI in terms of their dependence on r over a wide range. In this section, based on Sections IV-A–IV-D we also show the analytical results of $P_{\rm D}$ of the optimum receivers with the effects of diffusion noise and ISI produced by 1 and 5 previous bits, as shown in Fig. 6.

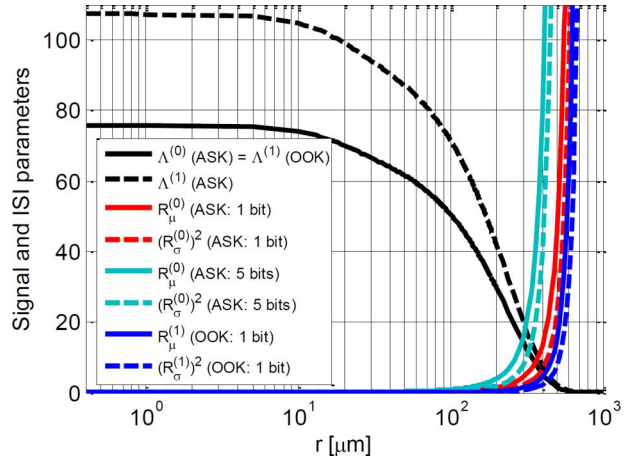

Fig. 5. Quantities related to and expressing signal and ISI statistics when $T_{\rm sym} = 100$ s. In the legends of Figs. 5 and 6, "1 bit" and "5 bits" denote the scenarios when ISI-producing molecules from the previous 1 and 5 bits are considered respectively.

1) Characteristics of Signal- and ISI-Related Quantities: As shown in Fig. 5, in short-range and medium range CEMC when $r \leq 10$ μm, Λ remains almost unchanged, while the quantities $R_\mu^{(i)}$ and $(R_\sigma^{(i)})^2$, $i \in \{0,1\}$, remain almost unchanged up to $r \leq 100$ μm. However, when $r > 10$ μm, Λ decreases, and when $r > 100$ μm, both $R_\mu^{(i)}$ and $(R_\sigma^{(i)})^2$, $i \in \{0,1\}$ increase. The quantity Λ represents signal to diffusion noise strength ratio. The decrease in Λ indicates the severity of diffusion-based noise when r increases. Regardless of mean signal strength and diffusion-noise, the values of $R_\mu^{(i)}$ and $(R_\sigma^{(i)})^2$, $i \in \{0,1\}$ depend on the ISI-producing molecules contributed from the previous symbols. Therefore, in order to see the detection performance, we consider two cases, where the ISI is produced by the residual molecules from the previous 1 and 5 bits. In the latter case, the effect of ISI is much, and so $P_{\rm D}$ provides degraded performance as shown in Fig. 6. The increasing trends of $R_\mu^{(i)}$ and $(R_\sigma^{(i)})^2$, $i \in \{0,1\}$, with the increase of communication range denote the fact that the effects of ISI are more severe at longer communication ranges. More importantly, another notable feature is that $R_\mu^{(i)} \approx (R_\sigma^{(i)})^2$, $i \in \{0,1\}$ when $r \leq 100$ μm, which provides us with the possible justification that a simpler version of suboptimum receiver, known as *Scenario 2*, can be made possible and is shown in Appendix B. When $r > 100$ μm, it is found that $R_\mu^{(i)} > (R_\sigma^{(i)})^2$, $i \in \{0,1\}$, which can be explained as follows: when $r > 100$ μm, the CIR spreads very much temporally, and so there occur more temporal samples with $p(t) > 0$ when $t \geq T_{\rm sym}$, and, therefore, when $t \geq T_{\rm sym}$, the effects

$$P_{\rm D} = \mathsf{Q}\left(\mathsf{Q}^{-1}(P_{\rm FA})\left(\frac{R_\mu^{(1)}}{1+R_\mu^{(1)}}\right)\frac{R_\sigma^{(1)}}{\sqrt{1+(R_\sigma^{(1)})^2}} - \frac{\Lambda^{(1)}}{2}\left\{\frac{1+2R_\mu^{(1)}}{\left(1+R_\mu^{(1)}\right)\sqrt{1+(R_\sigma^{(1)})^2}}\right\}\right)$$

$$\text{where } \Lambda^{(1)} = \frac{s_{\rm ED}^{(1)}}{\sigma_{\rm S(ED)}^{(1)}}, R_\mu^{(1)} = \frac{\mu_{\rm ISI(ED)}}{s_{\rm ED}^{(1)}}, R_\sigma^{(1)} = \frac{\sigma_{\rm ISI(ED)}}{\sigma_{\rm S(ED)}^{(1)}}. \tag{23}$$

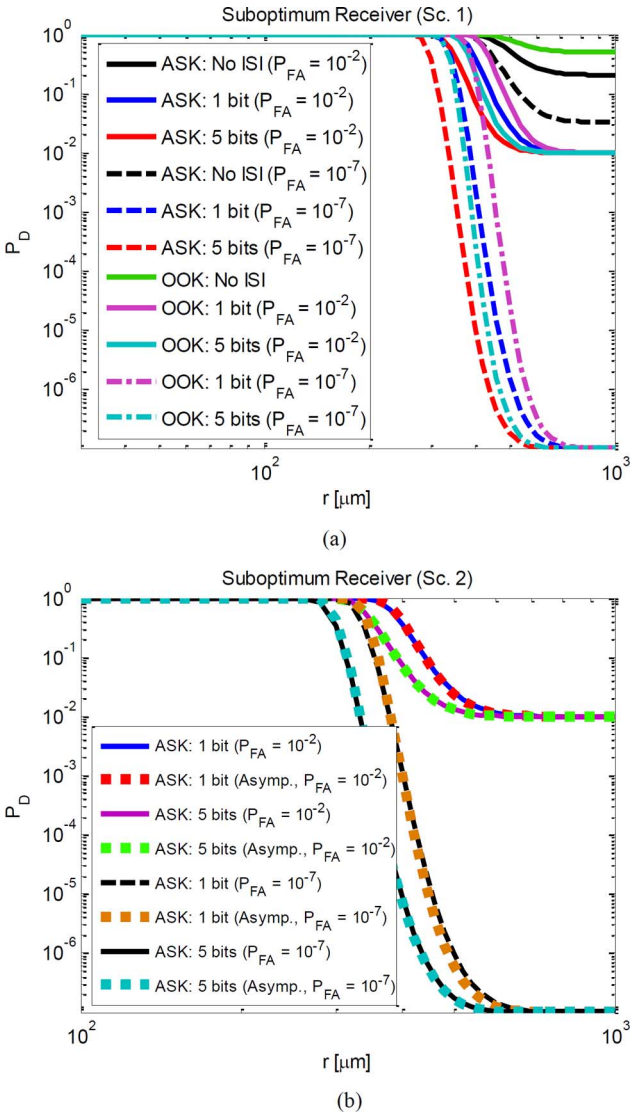

Fig. 6. $P_{\rm D}$ versus r characteristics of the suboptimum receivers: Scenario 1 in (a) and Scenario 2 in (b), in ISI-free and ISI-affected scenarios when $f = 0.01$ bps (i.e., $T_{\rm sym} = 100$ s), $\alpha = 2$, and $Q_0 = 5000$ molecules. ISI is produced by the previous 1 and 5 bits respectively. Note that $\Lambda^{(i)}, i = \{0, 1\}$, can be computed at each r. (a) Suboptimum receiver (*Scenario 1*); (b) Suboptimum receiver (*Scenario 2*).

of $\mu_{\rm ISI(ED)} > \sigma^2_{\rm ISI(ED)}$ becomes more dominant than that of $s_{\rm ED} > \sigma^2_{\rm S(ED)}$.

2) Detection Performance: The detection performances derived in (22), (23), and in Appendix B, are very useful in the sense that they offer the versatility of using $R_\mu^{(i)}$ and $(R_\sigma^{(i)})^2$, $i \in \{0, 1\}$ in studying the role of ISI in the system, e.g., as shown in Fig. 6 plugging $R_\mu^{(i)} = 0$ and $R_\sigma^{(i)} = 0$, $i \in \{0, 1\}$ would provide the detection performance in the ISI-free situation with the effects of diffusion-noise only and plugging any other values of $R_\mu^{(i)}$ and $R_\sigma^{(i)}$, $i \in \{0, 1\}$ would produce the detection performance correspondingly. As shown in Fig. 6, in the absence of ISI, $P_{\rm FA}$ does not affect $P_{\rm D}$ in OOK receiver, though it affects the same in ASK receiver, the reason being the fact that the ASK receiver sends Q_0 molecules even when it sends bit 0, causing a non-zero probability of false detection. In the absence of ISI, the OOK receiver provides superior performance to the ASK receiver. Here $P_{\rm D}$ increases as r decreases, meaning that, when r decreases, an improved signal to noise strength ratio provides better detection capabilities in both ISI-free and ISI-affected situations. Fig. 6(a) shows the detection performance of both ASK and OOK systems in three cases, namely, ISI-free and ISI from previous 1 bit and 5 bits when $P_{\rm FA} = 10^{-2}$ and 10^{-7}. As shown in Fig. 6(a), increased level of ISI produces a decrease in $P_{\rm D}$.

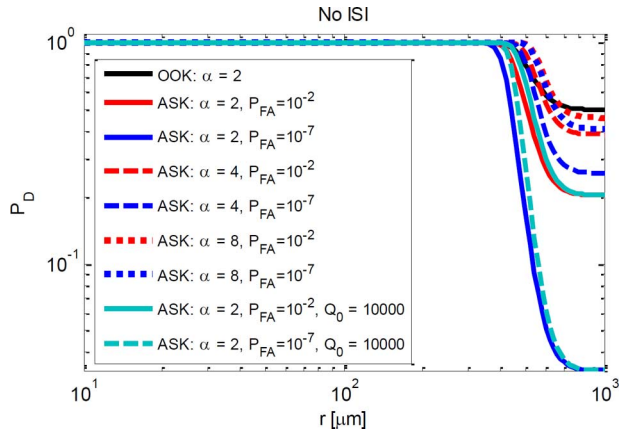

Fig. 7. Effects of α on $P_{\rm D}$ versus r characteristics when $f = 0.01$ bps (i.e., $T_{\rm sym} = 100$ s), $\alpha = 2$, 4, and 8, $Q_0 = 5000$ (not marked in the legend) and $Q_0 = 10000$ (marked in the legend) without the presence of ISI.

3) Role of the Strength Factor: The role that strength factor plays in the detection performance can be shown by varying either or both of α and Q_0. However, as shown in Fig. 7, in the absence of ISI the detection performance of the ASK receiver can be made even better than the OOK receiver if α is increased, e.g., from $\alpha = 2$ to $\alpha = 4$ or 8 at the TN when the remaining quantities are kept unchanged. On the other hand, increasing α and/or Q_0 can help increase the $P_{\rm D}$ even in presence of ISI; however, the results being straightforward and similar, the data for the ISI-affected scenario are not shown in this paper. In addition, note that in Fig. 5 to Fig. 7, the quantities showing the results have been computed when r varies from as short as 400 nm up to as long as 1000 μm and $T_{\rm sym} = 100$ s. For a different data rate (i.e., a different $T_{\rm sym}$), the quantities would change correspondingly, and so would the $P_{\rm D}$.

4) Asymptotic Performance: For the ASK system, the asymptotic behavior of the *exact* detection performance of the optimum receiver as shown in (18) is difficult to be found analytically, mainly due to its complicated structure. However, when $r \to 0$, $\mu_{\rm ISI} \to 0$ and $\sigma^2_{\rm ISI} \to 0$, and as a result, since $s^{(1)}_{\rm ED} = \alpha s^{(0)}_{\rm ED}$ and $\sigma^{2(1)}_{\rm ED} = \alpha \sigma^{2(0)}_{\rm S(ED)}$, it can be shown from (11) that $b_{\rm ED} \to 0$ and $a_{\rm ED} \to (1 - \alpha^{-1})/2\sigma^{2(0)}_{\rm S(ED)}$, and therefore, in the limit $r \to 0$, $c_{\rm ED} \to 0$, i.e., $\mathcal{L}_{r\to 0}[c_{\rm ED}] = 0$, where $\mathcal{L}$ denotes the limit operator. In addition, when $r \to 0$, since both $s^{(i)}_{\rm ED}$ and $\sigma^{2(i)}_{\rm S(ED)}$ are non-zero, this yields $R_\mu^{(i)} \to 0$ and $R_\sigma^{(i)} \to 0$, $i \in \{0, 1\}$.

On the other hand, as shown in Fig. 5, when $r \to \infty$, because of the diffusion process and the extremely large temporal spreading of the CIR, $\mu_{\rm ISI}$ and $\sigma^2_{\rm ISI}$ become very large and show asymptotic behavior when $r \to \infty$: $\mu_{\rm ISI} \to \infty$ and $\sigma^2_{\rm ISI} \to \infty$, and as a result, after plugging the expressions of $b_{\rm ED}$ and $a_{\rm ED}$ from (11) into $c_{\rm ED} = b_{\rm ED}/a_{\rm ED}$ and performing algebraic simplifications, it can be shown that $\mathcal{L}_{r\to\infty}[c_{\rm ED}] =$

$\mathcal{L}_{r\to\infty}[(1/a_{\mathrm{ED}})/(1/b_{\mathrm{ED}})] = 0$. In addition, when $r \to \infty$, both $s_{\mathrm{ED}}^{(i)}$ and $\sigma_{\mathrm{S(ED)}}^{2(i)}$ tend to zero, and so $R_{\mu}^{(i)} \to \infty$ and $R_{\sigma}^{(i)} \to \infty$, $i \in \{0,1\}$.

As a result, both the asymptotic cases, when $r \to 0$ and $r \to \infty$, allow us to show that the optimum receiver shown in (18) actually turns into a suboptimum receiver as shown in (22). Therefore, this also allows us to show the asymptotic detection performance of the suboptimum receiver shown in (22) to explain the same of the optimum receiver shown in (18). Applying these limiting conditions into (22) and (B.3) and simplifying the algebraic expressions, the asymptotic detection performance for the ASK system in Scenario 1 and Scenario 2 can be obtained as shown in (24).

$$\mathcal{L}_{r\to 0}[P_{\mathrm{D}}] = \begin{cases} \mathrm{Q}\left(\dfrac{\mathrm{Q}^{-1}(P_{\mathrm{FA}})}{\alpha^{3/2}} - \dfrac{\Lambda^{(0)}}{2}\left\{\dfrac{\alpha^2-1}{\alpha^{3/2}}\right\}\right) & (\text{Sc. 1: ASK}) \\ \mathrm{Q}\left(\dfrac{\mathrm{Q}^{-1}(P_{\mathrm{FA}})}{\alpha^{1/2}} - \Lambda^{(0)}\left\{\dfrac{\alpha-1}{\alpha^{1/2}}\right\}\right) & (\text{Sc. 2: ASK}) \end{cases}$$

$$\mathcal{L}_{r\to\infty}[P_{\mathrm{D}}] = \begin{cases} P_{\mathrm{FA}} & (\text{Sc. 1: ASK}) \\ P_{\mathrm{FA}} & (\text{Sc. 2: ASK}). \end{cases} \tag{24}$$

By applying a similar approach, the asymptotic performance of the OOK system can also be found. However, the approach being very straightforward, we have not shown that in this paper.

Note that, as shown in (24), when $r \to 0$, the asymptotic detection performance is affected much by $\Lambda^{(0)}$ and for the range of values of $\Lambda^{(0)}$ as shown in Fig. 5, this yields $P_{\mathrm{D}} \to 1$. On the other hand, when $r \to \infty$, in the case of suboptimum receiver, both in Scenario 1 and Scenario 2, see (22) and (B.3) respectively, since $R_{\mu}^{(i)} \to \infty$ and $R_{\sigma}^{(i)} \to \infty$, i.e., $1/R_{\mu}^{(i)} \to 0$ and $1/R_{\sigma}^{(i)} \to 0$, $i \in \{0,1\}$, after algebraic simplifications, P_{D} becomes independent of $\Lambda^{(0)}$ and equals the chosen value of P_{FA}. Such asymptotic results of P_{D} can be verified as shown in Fig. 6 when $r \to 0$ and $r \to \infty$.

As shown in (11), (17), (21), and (B.1), the mean and the variance of ISI-producing molecules originating from one or more of the previous bits, as estimated by the RN, can vary based on receiver memory and cause the detection threshold setting vary accordingly [45]. Therefore, in Figs. 6 and 7 we particularly focus on the P_{D} versus r characteristics for two P_{FA} settings, where at each r the signal to diffusion noise strength ratio Λ can be computed. And for equiprobable bits transmitted by the TN, when P_{D} and P_{FA} values are found from (22), (23), (B.3) and (B.4), BER can also be expressed as the following.

$$\mathrm{BER} = \frac{(1 - P_{\mathrm{D}}) + P_{\mathrm{FA}}}{2}. \tag{25}$$

For a given P_{FA}, BER decreases as P_{D} increases and vice versa. Therefore, keeping P_{FA} unchanged a detector that maximizes P_{D} would be highly desired. The most noteworthy feature of the detection performances of the optimum ASK and OOK receivers and their suboptimum versions in CEMC as shown in (18), (22), (23), (B.3), and (B.4) is that detection performances are affected by signal values themselves, unlike many traditional AWGN-affected communication signals, e.g., see [21]. Note that the variances of the diffusion noise in both H_1 and H_0 hypotheses are functions of the signal values themselves respectively [see (4)].

Comparing Fig. 6(a) with Fig. 6(b), the suboptimum receiver in Scenario 2 can effectively follow the similar curves for the same in Scenario 1. This implies, in Scenario 1, when $s_{\mathrm{ED}}^{(0)} \approx \sigma_{\mathrm{S(ED)}}^{2(0)}$, $s_{\mathrm{ED}}^{(1)} \approx \sigma_{\mathrm{S(ED)}}^{2(1)}$, and $\mu_{\mathrm{ISI(ED)}} \approx \sigma_{\mathrm{ISI(ED)}}^{2}$, it turns into the threshold-based receiver as shown in Scenario 2 in Appendix B [see (B.1)–(B.3)].

V. Simulation Results on Bit Error Rate

A. Simulation Setup

The purpose of simulation experiments used here is to test the functionality of the strength-based optimum receiver model thus developed at various system settings with sequences of randomly transmitted bits. Based on (11), the optimum and the suboptimum receivers for CEMC system have been implemented in software platform and tested using simulation experiments. We explain the optimum receiver in terms of three main factors, namely, communication range (r) and transmission data rate (f), and receiver memory size (M). The receivers thus developed have been evaluated by using Monte Carlo simulations with at least 10 000 and up to 100 000 randomly generated bits at each setting of the experiment and BER results are obtained [46]. Information molecules having a diffusion constant of 10^{-6} cm^2/s, i.e., 100 $\mu\mathrm{m}^2/\mathrm{s}$, in water medium has been assumed [47]. An observation time up to 10 000 000 simulated seconds ($\approx$ 2777 simulated hours) is considered. Here D is assumed to remain unchanged over the entire observation time [10]. Communication ranges from 400 nm up to 100 μm [10] covering short, medium, and long-range CEMC in water medium are considered with transmission data rates of 0.01 bits per second (bps) up to 0.1 bps [48]. In the ASK scheme, TN emits 5000 and 10 000 molecules when it wants to send bits 0 or 1 respectively, while in the OOK scheme, it sends 0 and 5000 molecules to send bits 0 and 1 respectively. These are feasible numbers of molecules to be released from a vesicle to generate a spike (impulse) [40], [42]. Each transmitted bit is tested by using 30 different randomly generated CIR realizations such that the probability that the sample mean of the CIR at the RN at time instant t differs from the true mean by less than one standard deviation is 0.96 [49]. Based on (1)–(7), the output concentration intensity signal is computed numerically by taking time domain convolution of the input transmission rate and the energy-normalized [18], [44] randomly generated CIR of the CEMC channel. A sampling-based receiver [18] has been considered here that samples the output concentration signal, i.e., senses the occupancy of its receptors, uniformly at intervals of 1 second (s) [10]. Based on the concept of an *ideal molecule* monitor [38], [39], [42], we consider the concentration of molecules, i.e., the number of molecules available per unit sensing volume of the RN.

B. Receiver Configurations

Based on RN's ability to estimate the ISI-producing molecules present at the current symbol, we consider three different receiver configurations at the RN as shown below.

First, in the *simplest receiver* configuration, the RN is so simple in its structure that it is not at all able to determine $\mu_{\mathrm{ISI(ED)}}$ and $\sigma_{\mathrm{ISI(ED)}}^2$ in the current symbol. Therefore, referring to (7), it assumes that on average one ISI-producing molecule (with unity variance) is present at the current symbol, i.e., $n_{\mathrm{ED}}^{\mathrm{ISI}} \sim \mathcal{N}\left(\mu_{\mathrm{ISI(ED)}}, \sigma_{\mathrm{ISI(ED)}}^2\right) = \mathcal{N}\left(1,1\right)$.

Due to the inherent nature of the diffusion process itself, in the ideal case, the molecules can arrive at the RN even after infinite time. In addition, in CEMC, the presence of a large number of molecules in the system makes it very likely that one or more molecules from the previous symbols can be present at the RN. Therefore, we investigate into the simplest receiver configuration where the RN assumes that a minimum level of ISI is present in the system where $n_{\mathrm{ED}}^{\mathrm{ISI}}$ is a normal-distributed random variable with unity mean and unity variance. Note that (4) shows the variance of concentration intensity affected by diffusion-noise.

In this configuration, the receiver is the simplest in terms of functional complexity required to detect the information symbols. This version of the receiver can be considered useful in view of the extremely limited tasks and capabilities of a nanomachine [5] such that the RN may not have the ability to compute the ISI-producing molecules at all. With the *simplest* receiver configuration, the RN does not have to estimate the ISI correctly on per symbol basis, nor maintain a memory of the previous symbols, which allows implementing the RN with the simplest receiver circuitry. Therefore, the RN can avoid complicated procedures to estimate ISI correctly, but acknowledges the effects of diffusion-noise by assuming that there is one ISI-producing molecule present with unity variance. The *simplest receiver* configuration might be useful when estimating ISI correctly at the RN through complicated signal processing techniques might not be necessary, depending on the communication range of operation, e.g., in short-range CEMC when attenuation and temporal spreading of concentration signal is found minimum at the RN [10], or when determining the ISI correctly might not be possible due to the limited capability of the RN itself.

Second, a *reduced complexity (RC) receiver* configuration computes the mean and the variance of ISI-producing molecules by using a number of previously transmitted symbols that is less than the total number of all previous symbols. To make an in-depth investigation, we assume 9 different settings of the RN based on the complexity of the RN, i.e., how many of the previous symbols would be processed by the RN in order to determine $\mu_{\mathrm{ISI(ED)}}$ and $\sigma^2_{\mathrm{ISI(ED)}}$ at the current symbol. For instance, at the i^{th} symbol, the *full complexity (FC) receiver* discussed in the next paragraph and the RC receiver discussed here compute $\mu_{\mathrm{ISI(ED)}}$ and $\sigma^2_{\mathrm{ISI(ED)}}$ by using *all of* $(i-1)$ and $\mathrm{M} < (i-1)$ previously transmitted bits respectively. When $\mathrm{M} = (i-1)$, the RC receiver turns into the FC receiver. Therefore, in terms of complexity in the RN circuitry, the RC receiver is comparatively simpler than the FC receiver. In the numerical experiments, the RN can determine $\mu_{\mathrm{ISI(ED)}}$ and $\sigma^2_{\mathrm{ISI(ED)}}$ at the current symbol by processing the previous $\mathrm{M} = 1, 2, 5, 10, 20, 40, 60, 80,$ and 99 symbols.

Finally, an FC receiver determines $\mu_{\mathrm{ISI(ED)}}$ and $\sigma^2_{\mathrm{ISI(ED)}}$ from all the previously transmitted bits and, as a result, the RN requires the most complex circuitry in this configuration to implement the detection functionality.

C. BER Performance

Despite its simple structure, the simplest receiver configuration has been found to detect the CEMC bits quite effectively. Fig. 8 shows the BER performance of the optimum and the suboptimum versions of ASK and OOK receivers at various communication ranges and data rates. As shown in Fig. 8, the suboptimum version of the receiver performs almost equally well as the optimum receiver. In other words, this means the approximation shown in Section IV-C can be considered as acceptable and thus provides with almost the same performance as the optimum receiver, even though the derivation of the exact detection performance shown in (18) seems quite difficult analytically.

As shown in Fig. 8(a), for data rates of 0.01 bps and 0.05 bps, the optimum ASK simplest receiver can detect all the bits correctly $(\mathrm{BER} = 0)$ up to 30 μm and 10 μm respectively, and beyond this range the BER increases as r increases, meaning that the higher transmission data rate suffers from higher BER at longer communication ranges. At higher data rates, symbol duration becomes shorter and the effect of ISI becomes dominant and hence an increased BER. Since the simplest receiver is not able to estimate the ISI accurately, this increases the BER. For example, when the transmission data rate increases to 0.1 bps, being closer to the TN does not help the RN to recover from the higher BER, and the performance degrades significantly causing approximately 22% of the bits to be detected erroneously when $r = 800$ nm. On the other hand, the suboptimum ASK receiver has been implemented by plugging $c_{\mathrm{ED}} = 0$ in (11) and thereby after implementing the resulting suboptimum receiver in software, the simulation results of the BER have been shown in Fig. 8(a). Results show that the suboptimum receiver is able to provide the BER performance almost the same as that of the optimum receiver. Finally, the comparison between the optimum and the suboptimum RC receivers with 1 and 5 bit memories has also been shown in Fig. 8(a). BER results show that the suboptimum RC receiver can perform reasonably well as the optimum receiver. In addition, the RC receiver provides less BER than the simplest receiver, which is because the RC receiver can estimate the ISI molecules with a better accuracy, while the simplest receiver cannot estimate that at all.

On the other hand, Fig. 8(b) shows the performances of the optimum and the suboptimum versions of the simplest and the RC receivers based on OOK modulation when $f = 0.05$ bps. As shown in Fig. 8(b), the *simplest* OOK receiver performs worse than the *simplest* ASK receiver shown in Fig. 8(a). This is because, in OOK, since the TN sends no molecules at all when it transmits bit 0, the simplest OOK receiver produces bit errors in the detection process, which can be explained from the values of the coefficients a_{ED}, b_{ED}, and γ_{ED} in (11) for OOK and ASK systems when $\mu_{\mathrm{ISI(ED)}} = 1$ and $\sigma^2_{\mathrm{ISI(ED)}} = 1$. This in turn suggests that the optimum OOK receiver based on the simplest receiver configuration should not be a good choice for CEMC, which necessitates an investigation into the optimum RC and FC receivers with a finite memory size, as shown in Fig. 9. In addition, Fig. 8(b) also shows that the suboptimum version of the OOK receiver provides reasonably consistent BER results like the optimum OOK receiver, which again suggests that the approximation of the optimum receiver to its suboptimum version is reasonably acceptable.

Finally, Fig. 8(c) shows the comparison between the optimum and the suboptimum receivers, as well as these and the theoretical BER performances at $P_{\mathrm{FA}} = 10^{-7}$ when ISI is considered to be produced from the previous 1 and 5 bits. At extended communication ranges beyond 100 μm, more specifically when $400\ \mu\mathrm{m} < r < 1000\ \mu\mathrm{m}$, the temporal spreading

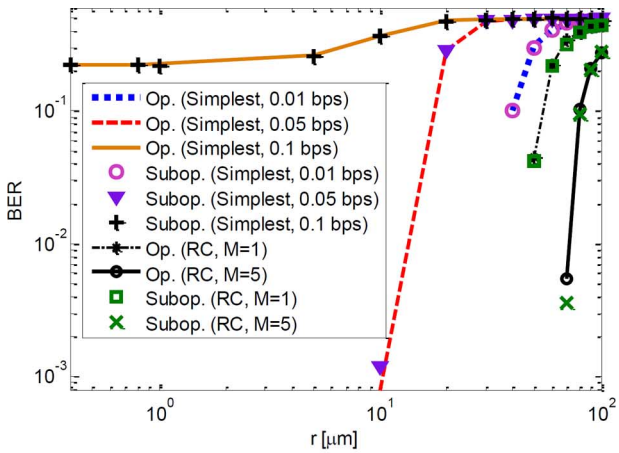

(a)

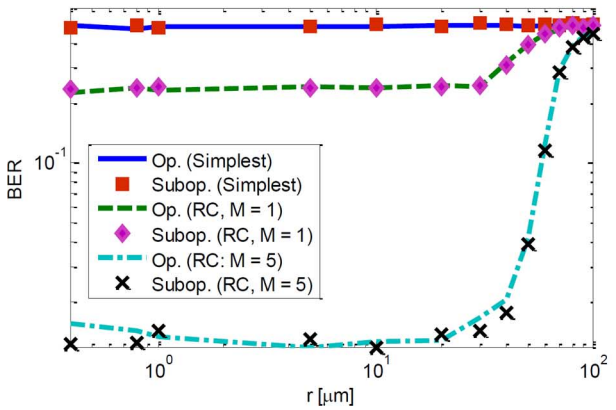

(b)

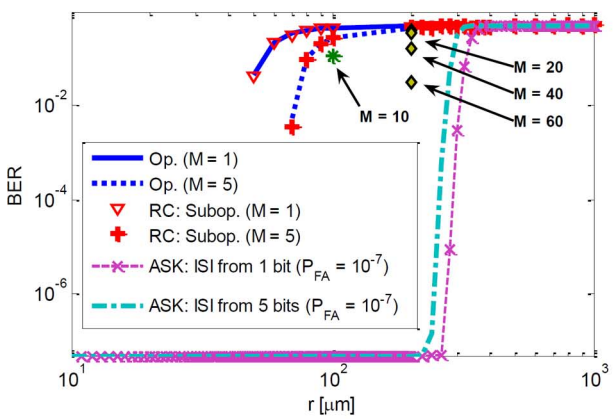

(c)

Fig. 8. BER Performance of the optimum and suboptimum versions of the *simplest* and the *reduced-complexity* (RC) receivers with (a) ASK modulation and (b) OOK modulation at various communication ranges and data rates, and (c) BER performance at extended communication ranges beyond 100 μm. (a) ASK modulation. (b) OOK modulation with $f = 0.05$ bps. (c) ASK modulation.

becomes so large that theoretical and simulation results coincide at BER $= 0.5$, i.e., a random guess. This can be explained from the analytical results as follows: when $r \to \infty$, from (24) $P_{\rm D} \to P_{\rm FA}$, and as a result from (25), BER $\to 0.5$. When $r < 200$ μm approximately, the theoretical BER performance depends on the allowed $P_{\rm FA}$ of the detector. For example, when

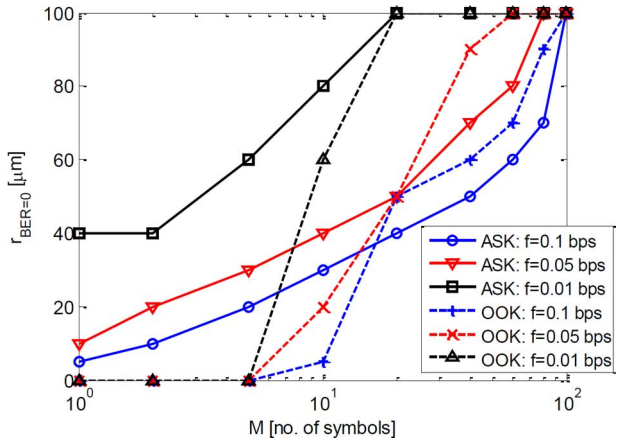

Fig. 9. Performance of the optimum RC receiver in terms of $r_{\rm BER=0}$ at various receiver memory sizes and transmission data rates.

$P_{\rm FA} = 10^{-7}$ and $r < 200$ μm, as shown from Figs. 6(a) and 6(b), $P_{\rm D} \approx 1$, and from (25), BER $\approx P_{\rm FA}/2$, which can be verified in Fig. 8(c).

Regarding the simulation results on BER, for the optimum RC receivers with M $= 1$ and M $= 5$, BER $= 0$ is found when $r < 50$ μm and $r < 70$ μm respectively, which is consistent with the theoretical results as shown in Fig. 8(c). However, when 50 μm $\leq r \leq$ 400 μm, the performances of the optimum and the suboptimum receivers compared to the corresponding theoretical results are mainly controlled by the RN's memory size. For instance, when $r = 100$ μm, an increase in M to M $= 10$ yields the BER as denoted by the green asterisk $(*)$, and M > 10 yields BER $= 0$. Similarly, when $r = 200$ μm, if M increases, BER decreases, as denoted by the diamond marks $(\blacklozenge)$ in Fig. 8(c) for M $= 20$, 40, and 60, where for M > 60, BER $= 0$ is achieved. Therefore, for 50 μm $\leq r \leq$ 400 μm, the simulation results on BER tend to match with the theoretical BER results if M increases. This is because when M increases, the RC receiver can estimate the ISI quantities $\mu_{\rm ISI(ED)}$ and $\sigma^2_{\rm ISI(ED)}$ reasonably accurately such that when the estimated values of $\mu_{\rm ISI(ED)}$ and $\sigma^2_{\rm ISI(ED)}$ are plugged into (11) in implementing the optimum receiver in software, the RC receiver provides less BER. Therefore, a larger receiver memory yields a close match between the simulation and the theoretical results for 50 μm $\leq r \leq$ 400 μm.

In addition, as shown in Fig. 8(c), the sharp increase in the theoretical BER when 200 μm $\leq r \leq$ 400 μm can be explained as follows: as shown in Fig. 5, when 200 μm $\leq r \leq$ 400 μm, for the ASK system the quantities $\Lambda^{(i)}$, $i \in \{0, 1\}$, decrease sharply, and on the other hand the quantities $R_\mu^{(i)}$, and $(R_\sigma^{(i)})^2$, $i \in \{0, 1\}$, increase sharply. When this happens, as shown in Section IV-C, a decrease in $\Lambda^{(i)}$, $i \in \{0, 1\}$, decreases the $P_{\rm D}$ and at the same time an increased level of ISI-producing molecules dominates and hence causes a decrease in $P_{\rm D}$, which finally yields BER $\to 0.5$ when $r \to \infty$. Note that the asymptotic performance of $P_{\rm D}$ when $r \to \infty$ is shown in (24).

As shown in Fig. 9, with the RC receiver, more reliable CEMC can be achieved for the OOK system at the cost of larger memory size at the RN. For example, when a bit sequence of length 100 is transmitted, M $= 99$ would indicate the FC receiver configuration when all the previous bits would be considered while determining the ISI statistics at the current

symbol. As a result, this yields zero BER. The effect of memory size of the receiver on the performance of optimum RC receiver has been shown in Fig. 9 in terms of the quantity $r_{\mathrm{BER}=0}$ that indicates the *communication range up to which zero BER can be obtained* for given memory size and transmission data rate. Thus, Fig. 9 shows how the performance of an RC receiver can be obtained by using a larger memory size when compared to the simplest receiver.

It is observed that with smaller memory size $\mathrm{M} < 20$, ASK system provides better BER performance than the OOK scheme, while the opposite is true when $\mathrm{M} > 20$. The crossover point in memory size is important because it shows that, at a given transmission data rate, the performances of the ASK and the OOK schemes change. In OOK system, at $\mathrm{M} < 20$, some of the bits get detected erroneously when both the current bit and all the M previous bits are 0s, thereby the optimum receiver finds $\mu_{\mathrm{ISI(ED)}} = 0$ and $\sigma^2_{\mathrm{ISI(ED)}} = 0$. When this happens, given $s^{(0)}_{\mathrm{ED}} = 0$ and $\sigma^{2(0)}_{\mathrm{S(ED)}} = 0$ in the case of OOK, in order to avoid *divide-by zero* problem in (11), the optimum receiver thus implemented switches from the RC receiver to the simplest receiver and hence results in an increased probability of erroneous detection of the current bit. Such a degraded performance in OOK can be overcome by increasing M, because it makes it more unlikely for all the M previous bits to be 0s at the same time.

Finally, the FC receiver can detect all the transmitted bits correctly over a wide communication range from 400 nm up to 100 μm when the transmission data rate varies from 0.01 bps up to 0.1 bps. Completely error-free communication using the FC receiver can be attributed to the fact that RN now determines the ISI statistics using all of the previously transmitted bits.

Note that the RC and the FC receivers assume that the RN can detect the previous M bits correctly and, based on that, computes the ISI statistics at the current symbol and then applies them to the detection signal processing unit of the optimum and the suboptimum receivers. Such a scenario is important because it provides the most achievable detection performances of the optimum and the suboptimum receivers when M varies. In more realistic scenarios, when one or more of the previously transmitted bits are detected incorrectly, it would impact the ISI statistics computed by the RN and so the BER performance of the system. However, we have not considered this in this paper.

Apart from this, since the receiver is based upon statistically independent, uncorrelated samples of the concentration signal intensity, the effect of sampling time t_{s} on the BER performance of the optimum receiver is worth investigating. Figs. 10(a) and 10(b) show the BER performances achieved by the optimum simplest receiver and the optimum RC receiver with $\mathrm{M} = 1$ respectively. Due to the very nature of the diffusion process itself, the CIR peaks at the RN at some time and decays gradually over time. When t_{s} increases, the RN samples the concentration intensity at longer temporal intervals. Since the CIR at a given r and time t is normalized to the total energy, i.e., the total number of molecules received during the entire observation time [18], [44], when t_{s} increases, the relative amplitudes of the normalized CIR at temporal sampling instants increase in magnitude. This spreads the CIR and hence the RN senses more ISI. As a result, when $t_{\mathrm{s}} > 1$ s, this produces higher BER to both ASK and OOK systems than that when $t_{\mathrm{s}} = 1$ s. In this paper, to ensure statistically independent, uncorrelated concentration samples, we have considered $t_{\mathrm{s}} \geq 1$ s at the RN [38], [39]. When t_{s} remains unchanged, the performance of the optimum RC receiver with $\mathrm{M} = 1$ is better than the optimum simplest receiver because the RC receiver can make a better estimate of the ISI in the system. Note that sampling intervals of $t_{\mathrm{s}} = 1$ s has been considered all through the paper except for Fig. 10 below where, in addition to $t_{\mathrm{s}} = 1$ s, $t_{\mathrm{s}} = 2$ s, 5 s, 10 s, 20 s, and 50 s have also been investigated.

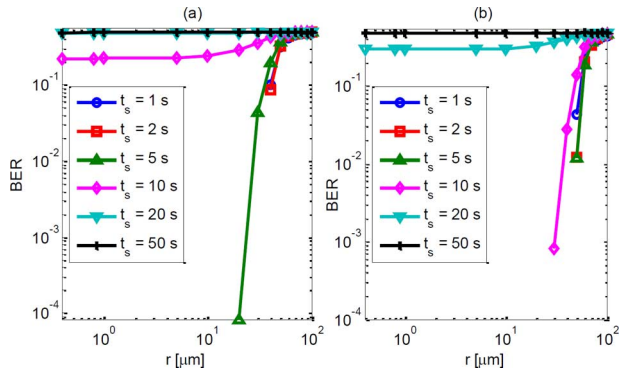

Fig. 10. Effects of sampling time on BER with the optimum *simplest receiver* in (a) and the optimum *RC receiver* with $\mathrm{M} = 1$ in (b) when $f = 0.01$ bps.

VI. Conclusion

In this paper, we have presented detailed theoretical formulations and architectures of the strength-based optimum receivers based on spike transmission of molecules. Expressions of detection probability of the suboptimum receivers have been derived analytically and explained in detail. The optimum and suboptimum versions of ASK and OOK receivers have also been implemented in software and their BER performances, based on three receiver configurations (the simplest, RC, and FC), have been evaluated through simulation experiments.

Although the current focus of the paper is mainly on spike (or impulse)-based modulation in binary CEMC, the receiver model developed in this paper can be applied to detect multilevel (M-ary) and pulse amplitude modulated (PAM) CEMC signaling by properly modifying the signal processing blocks of the optimum receiver. Although it is already known that bio-nanomachines, e.g., biological cells, can sense the concentration of molecules continually at their receptors [38] and biological cells can be engineered in order to do required tasks [7], the actual implementation of the strength-based detector at the cell level still requires a considerable amount of interdisciplinary research at the crossroads of molecular and synthetic biology, information theory, and communication engineering. In this paper, since our principal objective was to develop a fundamental structure of the optimum detector, given extremely limited functional complexity and computational burden of natural bio-nanomachines, [5], [8] we have not focused on addressing the challenges of a further computationally efficient detector circuitry at the RN with either higher number of samples per symbol or non-uniform (variable) sampling intervals, which we consider as future directions of this research. We strongly believe that the strength-based detection models presented in this paper should be useful in the study of the design of CEMC systems in greater details.

APPENDIX A
PROPERTIES OF MEAN AND VARIANCE OF TEST STATISTIC

At both H_0 and H_1 respectively, $\mu_{T''(\mathrm{H}_0)} \gg 1$, $\sigma^2_{T''(\mathrm{H}_0)} \gg 2$ and $\mu_{T''(\mathrm{H}_1)} \gg 1$ and $\sigma^2_{T''(\mathrm{H}_1)} \gg 2$.

Explanation With Biological Relevance: When $t_s \leq 1$ s, using (5), since $p(nt_s) \geq 0$, it can be shown that $s^{(1)}_{\mathrm{ED}} \geq \sigma^{2(1)}_{\mathrm{S(ED)}}$, $s^{(0)}_{\mathrm{ED}} \geq \sigma^{2(0)}_{\mathrm{S(ED)}}$, and $\mu_{\mathrm{ISI(ED)}} \geq \sigma^2_{\mathrm{ISI(ED)}}$. Hence, considering the above inequalities in (14) and (15), the following can be found for ASK and OOK systems respectively. See equation at the bottom of the page.

For instance, in (14), $\mu_{T''(\mathrm{H}_0)}$ will be minimum when $s^{(0)}_{\mathrm{ED}} = \sigma^{2(0)}_{\mathrm{S(ED)}}$, $\mu_{\mathrm{ISI(ED)}} = \sigma^2_{\mathrm{ISI(ED)}}$, and $c_{\mathrm{ED}} = 0$, and so $\min[\mu_{T''(\mathrm{H}_0)}] = s^{(0)}_{\mathrm{ED}} + \mu_{\mathrm{ISI(ED)}}$. In a CEMC system, a TN, e.g., a biological nanomachine, can send a large number of molecules contained in a vesicle [47] to transmit different information symbols. A typical vesicle can contain as many as several thousands of molecules in it [40], [42]. Therefore, when the strength of symbol is found based on (5), with $Q_{\mathrm{m}} \gg 1$ as large as the number of molecules inside a vesicle, it yields that the quantities $s^{(0)}_{\mathrm{ED}}$, $s^{(1)}_{\mathrm{ED}}$ and $\mu_{\mathrm{ISI(ED)}}$ are all reasonably large numbers, $\gg 1$, and hence $s^{(0)}_{\mathrm{ED}} + \mu_{\mathrm{ISI(ED)}} \gg 1$. Please note that the values of the quantities $s^{(0)}_{\mathrm{ED}}$, $s^{(1)}_{\mathrm{ED}}$, and $\mu_{\mathrm{ISI(ED)}}$ are directly linked with the biological fact of vesicles containing thousands of molecules. An artificial and/or engineered vesicle that would contain the required large number of molecules in it can also be built [7]. Since $\mathcal{X}^2_1$ has mean 1 and variance 2, the means and the variances of the test statistics above have been compared with 1 and 2 respectively.

On the other hand, when $t_s > 1$ s, since $p(nt_s) \geq 0$ is still valid, as shown in (5), the relationships between $s^{(i)}_{\mathrm{ED}}$ and $\sigma^{2(i)}_{\mathrm{S(ED)}}$ and $\mu_{\mathrm{ISI(ED)}}$ and $\sigma^2_{\mathrm{ISI(ED)}}$ depend on the factor $t_s^2(1-p(nt_s))$ and its relationship with t_s. When $t_s \gg 1$ s, $t_s^2(1-p(nt_s)) > t_s$, and yields $s^{(1)}_{\mathrm{ED}} < \sigma^{2(1)}_{\mathrm{S(ED)}}$, $s^{(0)}_{\mathrm{ED}} < \sigma^{2(0)}_{\mathrm{S(ED)}}$, and $\mu_{\mathrm{ISI(ED)}} < \sigma^2_{\mathrm{ISI(ED)}}$. In addition, it can be understood that when r is small, $s^{(i)}_{\mathrm{ED}} > \mu_{\mathrm{ISI(ED)}}$ and $\sigma^{2(i)}_{\mathrm{S(ED)}} > \sigma^2_{\mathrm{ISI(ED)}}$, whereas at large r, $s^{(i)}_{\mathrm{ED}} < \mu_{\mathrm{ISI(ED)}}$ and $\sigma^{2(i)}_{\mathrm{S(ED)}} < \sigma^2_{\mathrm{ISI(ED)}}$, $i \in \{0,1\}$. Hence, for instance, when r is small and large respectively, considering the above inequalities when $t_s > 1$ s, using (5), (14) and (15), and applying algebraic simplifications, it can be shown that

$$\mathrm{ASK}\begin{cases}\left.\begin{aligned}&\mu_{T''(H_i)} \geq \mathcal{K}^{(i)}_{\mu:(\text{Small } r)} \frac{s^{2(i)}_{\mathrm{ED}}}{\sigma^{2(i)}_{\mathrm{S(ED)}}} \gg 1\\ &\sigma^2_{T''(H_i)} \geq 4\mathcal{K}^{(i)}_{\sigma:(\text{Small } r)} \frac{s^{2(i)}_{\mathrm{ED}}}{\sigma^{2(i)}_{\mathrm{S(ED)}}} \gg 2\end{aligned}\right\} (\text{Small } r)\\ \left.\begin{aligned}&\mu_{T''(H_i)} \geq \mathcal{K}^{(i)}_{\mu:(\text{Large } r)} \frac{\mu^2_{\mathrm{ISI(ED)}}}{\sigma^2_{\mathrm{ISI(ED)}}} \gg 1\\ &\sigma^2_{T''(H_i)} \geq 4\mathcal{K}^{(i)}_{\sigma:(\text{Large } r)} \frac{\mu^2_{\mathrm{ISI(ED)}}}{\sigma^2_{\mathrm{ISI(ED)}}} \gg 2\end{aligned}\right\} (\text{Large } r)\end{cases}$$

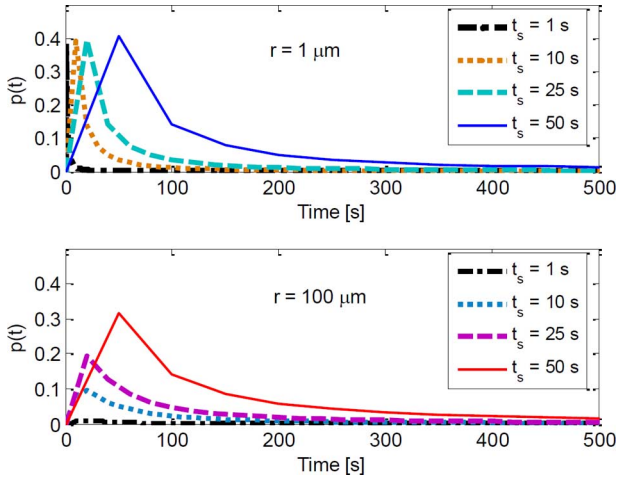

Fig. 11. Variation of $p(t)$ as a function of time for different t_s when $r = 1$ μm (top) and $r = 100$ μm (bottom) respectively.

where $\mathcal{K}^{(i)}_{\mu:(\text{Small } r)}$, $\mathcal{K}^{(i)}_{\sigma:(\text{Small } r)}$, $\mathcal{K}^{(i)}_{\mu:(\text{Large } r)}$, and $\mathcal{K}^{(i)}_{\sigma:(\text{Large } r)}$ are constants related to mean and variance of $T''(\mathrm{H}_i)$ when r is small and large respectively. The explanation and the justification above offers an opportunity to simplify the test statistic as shown in Section IV-B.

APPENDIX B
SUBOPTIMUM RECEIVERS (SCENARIO 2): APPROXIMATIONS TO $\mathrm{P_D}$ AT LONG RANGES AND/OR LONG TEMPORAL INSTANTS

When transmission data rates are in the range from $f = 0.01$ bps to 0.1 bps as shown in Section V, in general, the symbol intervals T_{sym} can be much larger than the r.m.s. delay spread τ_{DS}[50] of the channel. Hence, such cases may arise when long ranges or long temporal instants may cause $p(t) \approx 0$. As a result, the value of $p(t)$ can be considered as an indicative factor to possible detection scenarios. For instance, when $p(t) \approx 0$, it may refer to long-range CEMC with reduced complexity in the design of RN possible. When $p(t) \approx 0$, from (4), at any time instant t the intensity of molecular concentration can be expressed as $\mathcal{N}(s(t), s(t))$. Since in most realistic scenarios, when sampling intervals vary between 1 s and 50 s, as shown in Fig. 11, $0 \leq p(t) \leq 0.5$, $p(t) \to 0$ as $t \to \infty$, and symbol duration can be considered long enough, e.g., $T_{\mathrm{sym}} \gg \tau_{\mathrm{DS}}$, which results in $p(t) \approx 0$ at long temporal instants, this would overestimate the variance of signal intensity at the temporal samples in the earlier part of the symbol interval, where in reality the variance of signal intensity is smaller than its mean. However, as $t \to \infty$, the variance of signal intensity approaches its mean. Considering $p(t) \approx 0$ yields $s^{(0)}_{\mathrm{ED}} \approx \sigma^{2(0)}_{\mathrm{S(ED)}}$, $s^{(1)}_{\mathrm{ED}} \approx \sigma^{2(1)}_{\mathrm{S(ED)}}$, and $\mu_{\mathrm{ISI(ED)}} \approx \sigma^2_{\mathrm{ISI(ED)}}$, which as a result provides that $c_{\mathrm{ED}} \approx 0$

$$\mathrm{ASK}\begin{cases}\mu_{T''(\mathrm{H}_0)} \geq (s^{(0)}_{\mathrm{ED}} + \mu_{\mathrm{ISI(ED)}}) \gg 1 & \sigma^2_{T''(\mathrm{H}_0)} \geq 4\,(s^{(0)}_{\mathrm{ED}} + \mu_{\mathrm{ISI(ED)}}) \gg 2\\ \mu_{T''(\mathrm{H}_1)} \geq (s^{(1)}_{\mathrm{ED}} + \mu_{\mathrm{ISI(ED)}}) \gg 1 & \sigma^2_{T''(\mathrm{H}_1)} \geq 4\,(s^{(1)}_{\mathrm{ED}} + \mu_{\mathrm{ISI(ED)}}) \gg 2\end{cases}$$

$$\mathrm{OOK}\begin{cases}\mu_{T''(\mathrm{H}_0)} \geq \mu_{\mathrm{ISI(ED)}} \gg 1 & \sigma^2_{T''(\mathrm{H}_0)} \geq 4\mu_{\mathrm{ISI(ED)}} \gg 2\\ \mu_{T''(\mathrm{H}_1)} \geq (s^{(1)}_{\mathrm{ED}} + \mu_{\mathrm{ISI(ED)}}) \gg 1 & \sigma^2_{T''(\mathrm{H}_1)} \geq 4(s^{(1)}_{\mathrm{ED}} + \mu_{\mathrm{ISI(ED)}}) \gg 2.\end{cases}$$

$$P_{\mathrm{D}} = \mathsf{Q}\left(\frac{\sqrt{\sigma^{2(0)}_{\mathrm{S(ED)}} + \sigma^{2}_{\mathrm{ISI(ED)}}}}{\sqrt{\sigma^{2(1)}_{\mathrm{S(ED)}} + \sigma^{2}_{\mathrm{ISI(ED)}}}}\mathsf{Q}^{-1}(P_{\mathrm{FA}}) - \frac{s^{(1)}_{\mathrm{ED}} - s^{(0)}_{\mathrm{ED}}}{\sqrt{\sigma^{2(1)}_{\mathrm{S(ED)}} + \sigma^{2}_{\mathrm{ISI(ED)}}}}\right) \tag{B.2}$$

(since $b_{\mathrm{ED}} \approx 0$ and $a_{\mathrm{ED}} \neq 0$). The importance of $T_{\mathrm{sym}} \gg \tau_{\mathrm{DS}}$ is that it determines the severity of ISI in the system. The quantity $p(t)$ is important in the sense that MC system designers have the option to consider approximations in the system based on $p(t)$.

As a result, applying $c_{\mathrm{ED}} \approx 0$ in (13), we find that the suboptimum detector in this case becomes a threshold detector [20] as follows.

$$T'(z_{\mathrm{ED}}) = z_{\mathrm{ED}} \underset{\text{Select } \mathrm{H}_0}{\overset{\text{Select } \mathrm{H}_1}{\gtrless}} \gamma'^{(\mathrm{Threshold})}_{\mathrm{ED}} \text{ where}$$
$$\gamma'^{(\mathrm{Threshold})}_{\mathrm{ED}} = \sqrt{\gamma'_{\mathrm{ED}}}. \tag{B.1}$$

As reported in one of our previous works in [20], the detection performance of a threshold detector in CEMC can be expressed as (B.2) at the top of the page, that can be used to express the detection performance in terms of the ISI-related quantities as the following.

$$P_{\mathrm{D}} = \mathsf{Q}\left(\mathsf{Q}^{-1}(P_{\mathrm{FA}})\sqrt{\frac{1+(R^{(0)}_{\sigma})^2}{\alpha+(R^{(0)}_{\sigma})^2}} - \Lambda^{(0)}\frac{(\alpha-1)}{\sqrt{\alpha+(R^{(0)}_{\sigma})^2}}\right) \tag{B.3}$$

where $s^{(1)}_{\mathrm{ED}} = \alpha s^{(0)}_{\mathrm{ED}}$, $\sigma^{2(1)}_{\mathrm{S(ED)}} = \alpha\sigma^{2(0)}_{\mathrm{S(ED)}}$, and $R^{(0)}_{\sigma} = \sigma_{\mathrm{ISI(ED)}}/\sigma^{(0)}_{\mathrm{S(ED)}}$.

However, note that in this scenario $\Lambda^{(0)} = s^{(0)}_{\mathrm{ED}}/\sigma^{(0)}_{s} \approx \sqrt{s^{(0)}_{\mathrm{ED}}}$. Note that (B.3) differs from (22) in that it does not have $R^{(i)}_{\mu}$ terms because in the suboptimum threshold detector [20] the RN simply compares the strength z_{ED} of the symbol with the threshold without further processing it to derive the test statistic of the optimum receiver or the suboptimum version of the receiver in Scenario 1, see Equation (11), and hence the mean of ISI gets eliminated in the detection performance [20].

In OOK, since $s^{(0)}_{\mathrm{ED}} = 0$ and $\sigma^{2(0)}_{\mathrm{s(ED)}} = 0$, in a scenario just above, following a similar approach yields the detection performance as shown below

$$P_{\mathrm{D}} = \mathsf{Q}\left(\mathsf{Q}^{-1}(P_{\mathrm{FA}})\frac{R^{(1)}_{\sigma}}{\sqrt{1+(R^{(1)}_{\sigma})^2}} - \frac{\Lambda^{(1)}}{\sqrt{1+(R^{(1)}_{\sigma})^2}}\right) \tag{B.4}$$

where $\Lambda^{(1)} = s^{(1)}_{\mathrm{ED}}/\sigma^{(1)}_{\mathrm{S(ED)}}$ and $R^{(1)}_{\sigma} = \sigma_{\mathrm{ISI(ED)}}/\sigma^{(1)}_{\mathrm{S(ED)}}$.

Here, the signal strength to noise strength ratio can be given as $\Lambda^{(1)} = s^{(1)}_{\mathrm{ED}}/\sigma^{(1)}_{\mathrm{S}} \approx \sqrt{s^{(1)}_{\mathrm{ED}}}$.

ACKNOWLEDGMENT

The authors would like to thank the anonymous reviewers for providing very constructive feedback on the paper.

REFERENCES

[1] S. Hiyama, Y. Moritani, T. Suda, R. Egashira, A. Enomoto, M. Moore, and T. Nakano, "Molecular communication," in *Proc. NSTI Nanotechnol. Conf.*, 2005.
[2] T. Suda, M. Moore, T. Nakano, R. Egashira, and A. Enomoto, "Exploratory research on molecular communication between nanomachines," in *Genetic and Evolutionary Computation Conf. (GECCO), Late Breaking Papers*, Washington, DC, USA, Jun. 25–29, 2005.
[3] T. Nakano, T. Suda, M. Moore, R. Egashira, A. Enomoto, and K. Arima, "Molecular communication for nanomachines using intercellular calcium signaling," in *Proc. 5th IEEE Conf. Nanotechnol.*, 2005, vol. 2., pp. 478–481.
[4] M. J. Moore, A. Enomoto, T. Suda, T. Nakano, and Y. Okaie, "Molecular communication: New paradigm for communication among nanoscale biological machines," in *The Handbook of Computer Networks*, H. Bidgoli, Ed. New York: Wiley, 2007.
[5] I. F. Akyildiz, F. Brunetti, and C. Blazquez, "Nanonetworks: A new communication paradigm," *Comput. Networks J.*, vol. 52, pp. 2260–2279, 2008.
[6] T. Nakano, M. J. Moore, F. Wei, A. V. Vasilakos, and J. Shuai, "Molecular communication and networking: Opportunities and challenges," *IEEE Trans. NanoBiosci.*, vol. 11, pp. 135–148, 2012.
[7] T. Nakano, M. Moore, A. Enomoto, and T. Suda, "Molecular communication technology as a biological ICT," in *Biological Functions for Inform. and Communication Technologies*, H. Sawai, Ed. Berlin / Heidelberg, Germany: Springer-Verlag, 2011, pp. 49–86.
[8] T. Nakano, A. W. Eckford, and T. Haraguchi, *Molecular Communication*. Cambridge, U.K.: Cambridge Univ. Press, 2013.
[9] M. U. Mahfuz, D. Makrakis, and H. T. Mouftah, "Characterization of molecular communication channel for nanoscale networks," in *Proc. 3rd Int. Conf. Bio-Inspired Syst. Signal Process. (BIOSIGNALS-2010)*, Valencia, Spain, 2010, pp. 327–332.
[10] M. U. Mahfuz, D. Makrakis, and H. T. Mouftah, "On the characterization of binary concentration-encoded molecular communication in nanonetworks," *Nano Commun. Netw. J.*, vol. 1, pp. 289–300, 2010.
[11] A. Einstein, "On the movement of small particles suspended in stationary liquids required by the molecular-kinetic theory of heat," *Annalen Der Physik*, vol. 17, pp. 549–560, 1905.
[12] H. C. Berg, *Random Walks in Biology*. Princeton, NJ, USA: Princeton Univ. Press, 1993.
[13] A. W. Eckford, "Achievable information rates for molecular communication with distinct molecules," in *Bio-Inspired Models of Network, Inform. and Computing Systems*, ser. Lecture Notes of the Institute for Computer Sciences, Social Informatics and Telecommunications Engineering, 2nd ed. New York: Springer, 2007, vol. 39, pp. 313–315.
[14] M. U. Mahfuz, D. Makrakis, and H. T. Mouftah, "A comprehensive study of concentration-encoded unicast molecular communication with binary pulse transmission," in *Proc. 11th IEEE Conf. Nanotechnol. (IEEE-NANO),* , 2011, pp. 227–232.
[15] B. Atakan, S. Galmes, and O. Akan, "Nanoscale communication with molecular arrays in nanonetworks," *IEEE Trans. NanoBiosci.*, vol. 11, no. 2, pp. 149–160, Jun. 2012.
[16] K. V. Srinivas, A. W. Eckford, and R. S. Adve, "Molecular communication in fluid media: The additive inverse gaussian noise channel," *IEEE Trans. Inf. Theory*, vol. 58, pp. 4678–4692, 2012.
[17] M. U. Mahfuz, D. Makrakis, and H. Mouftah, "Spatiotemporal distribution and modulation schemes for concentration-encoded medium-to-long range molecular communication," in *Proc. 25th Biennial Symp. Commun. (QBSC)*, 2010, pp. 100–105.
[18] M. U. Mahfuz, D. Makrakis, and H. T. Mouftah, "Sampling based optimum signal detection in concentration-encoded molecular communication receiver architecture and performance," in *Proc. 6th Int. Conf. Bio-Inspired Syst. Signal Process. (BIOSIGNALS-2013)*, Barcelona, Spain, 2013.

[19] M. U. Mahfuz, D. Makrakis, and H. T. Mouftah, "Strength based receiver architecture and communication range and rate dependent signal detection characteristics of concentration encoded molecular communication," in *Proc. BWCCA-2012*, Victoria, BC, Canada, 2012, pp. 28–35.

[20] M. U. Mahfuz, D. Makrakis, and H. T. Mouftah, "A generalized strength-based signal detection model for concentration-encoded molecular communication," in *Proc. 8th Int. Conf. Body Area Netw. (BodyNets 2013)*, Boston, MA, USA, Sep.–Oct. 30–02, 2013, pp. 461–467.

[21] S. M. Kay, *Fundamentals of Statistical Signal Processing, Detection Theory*. Englewood Cliffs, NJ, USA: PTR Prentice-Hall, 1993, vol. 2.

[22] M. U. Mahfuz, D. Makrakis, and H. T. Mouftah, "On the detection of binary concentration-encoded unicast molecular communication in nanonetworks," in *Proc. 4th Int. Conf. Bio-Inspired Syst. Signal Process. (BIOSIGNALS-2011)*, Rome, Italy, Jan. 26–29, 2011, pp. 446–449.

[23] D. T. Gillespie, "The chemical Langevin equation," *J. Chem. Phys.*, vol. 113, pp. 297–306, Jul. 2000.

[24] M. U. Mahfuz, D. Makrakis, and H. T. Mouftah, "Strength-based optimum signal detection in concentration-encoded pulse-transmitted OOK molecular communication with stochastic ligand-receptor binding," *Simul. Modelling Practice Theory*, vol. 42, pp. 189–209, 2014.

[25] I. Llatser, A. Cabellos-Aparicio, M. Pierobon, and E. Alarcon, "Detection techniques for diffusion-based molecular communication," *IEEE J. Select. Areas Commun.*, vol. 31, pp. 726–734, 2013.

[26] D. Kilinc and O. B. Akan, "Receiver design for molecular communication," *IEEE J. Select. Areas Commun.*, vol. 31, pp. 705–714, 2013.

[27] S. Schuster, M. Marhl, and T. Höfer, "Modelling of simple and complex calcium oscillations," *Eur. J. Biochem.*, vol. 269, pp. 1333–1355, 2002.

[28] C. Schofl, G. Brabant, R. D. Hesch, A. v. z. Muhlen, P. H. Cobbold, and K. S. Cuthbertson, "Temporal patterns of alpha 1-receptor stimulation regulate amplitude and frequency of calcium transients," *Amer. J. Physiol. Cell Physiol.*, vol. 265, pp. C1030–C1036, 1993.

[29] K. Prank, F. Gabbiani, and G. Brabant, "Coding efficiency and information rates in transmembrane signaling," *BioSystems*, vol. 55, pp. 15–22, 2000.

[30] L.-S. Meng, P.-C. Yeh, K.-C. Chen, and I. F. Akyildiz, "A diffusion-based binary digital communication system," in *Proc. IEEE Int. Conf. Commun. (ICC)*, 2012, pp. 4985–4989.

[31] L.-S. Meng, P.-C. Yeh, K.-C. Chen, and I. F. Akyildiz, "Optimal detection for diffusion-based communications in the presence of ISI," in *Proc. IEEE Global Commun. Conf. (GLOBECOM)*, 2012, pp. 3819–3824.

[32] H. ShahMohammadian, G. G. Messier, and S. Magierowski, "Optimum receiver for molecule shift keying modulation in diffusion-based molecular communication channels," *Nano Commun. Netw.*, vol. 3, pp. 183–195, 2012.

[33] W.-A. Lin, Y.-C. Lee, P.-C. Yeh, and C.-h. Lee, "Signal detection and ISI cancellation for quantity-based amplitude modulation in diffusion-based molecular communications," in *Proc. IEEE Global Commun. Conf. (GLOBECOM)*, 2012, pp. 4362–4367.

[34] M. Pierobon and I. F. Akyildiz, "Diffusion-based noise analysis for molecular communication in nanonetworks," *IEEE Trans. Signal Process.*, vol. 59, pp. 2532–2547, 2011.

[35] S. Haykin, *Signals and Systems*. New York: Wiley, 2002.

[36] B. Atakan and O. B. Akan, "Deterministic capacity of information flow in molecular nanonetworks," *Nano Commun. Netw.*, vol. 1, pp. 31–42, 2010.

[37] B. Atakan, *Molecular Communications and Nanonetworks: From Nature to Practical Systems*. New York: Springer, 2014.

[38] H. C. Berg and E. M. Purcell, "Physics of chemoreception," *Biophys. J.*, vol. 20, pp. 193–219, 1977.

[39] R. G. Endres and N. S. Wingreen, "Accuracy of direct gradient sensing by single cells," *Proc. Natl. Acad. Sci. U. S. A.*, vol. 105, pp. 15749–15754, Oct. 2008.

[40] M. J. Moore, T. Nakano, A. Enomoto, and T. Suda, "Measuring distance from single spike feedback signals in molecular communication," *IEEE Trans. Signal Process.*, vol. 60, pp. 3576–3587, 2012.

[41] M. J. Moore and T. Nakano, "Synchronization of inhibitory molecular spike oscillators," *Proc. BIONETICS-2011*.

[42] M. J. Moore and T. Nakano, "Oscillation and synchronization of molecular machines by the diffusion of inhibitory molecules," *IEEE Trans. Nanotechnol.*, vol. 12, pp. 601–608, 2013.

[43] M. J. Moore, Y. Okaie, and T. Nakano, "Diffusion-based multiple access by nano-transmitters to a micro-receiver," *IEEE Commun. Lett.*, vol. 18, pp. 385–388, 2014.

[44] M. U. Mahfuz, D. Makrakis, and H. T. Mouftah, "Performance analysis of convolutional coding techniques in diffusion-based concentration-encoded PAM molecular communication systems," *BioNanoScience*, vol. 3, pp. 270–284, 2013.

[45] H. L. Van Trees, *Detection, Estimation, and Modulation Theory*. New York: Wiley, 1968-71.

[46] W. H. Tranter, *Principles of Communication Systems Simulation with Wireless Applications*. Upper Saddle River, NJ, USA: Prentice-Hall Professional Technical Reference, 2004.

[47] B. Alberts, A. Johnson, J. Lewis, M. Raff, K. Roberts, and P. Walter, *Molecular Biology of the Cell*. New York: Garland Science, 2008.

[48] M. U. Mahfuz, D. Makrakis, and H. T. Mouftah, "Transient characterization of concentration-encoded molecular communication with sinusoidal stimulation," in *Proc. 4th Int. Symp. Appl. Sci. Biomed. Commun. Technol. (ISABEL '11), Article 14*, Barcelona, Spain, 2011.

[49] A. Leon-Garcia, *Probability and Random Processes for Electrical Engineering*. Reading, MA, USA: Addison-Wesley, 1994.

[50] T. S. Rappaport, *Wireless Communications: Principles and Practice*. Upper Saddle River, NJ, USA: Prentice-Hall PTR, 2002.

[51] S. Haykin, *Communication Systems*. New York: Wiley, 2000.